Impacts of Inter-basin Water Diversion Projects on the Feedback Loops of Water Supply-Hydropower Generation-Environment Conservation Nexus

Jiaoyang Wang[1], Dedi Liu[1, 2, 3], Shenglian Guo[1], Lihua Xiong [1], Pan Liu [1], Hua Chen [1], Jie Chen [1], Jiabo Yin [1, 2], and Yuling Zhang[1]

[1] State Key Laboratory of Water Resources Engineering and Management, Wuhan University, Wuhan 430072, China

[2] Hubei Provincial Key Lab of Water System Science for Sponge City Construction, Wuhan University, Wuhan, 430072, China

[3] Department of Earth Science, University of the Western Cape, Bellville, Republic of South Africa.

Correspondence: Dedi Liu (dediliu@whu.edu.cn)

Abstract. To balance water resource distribution among different areas, inter-basin water diversion projects (IWDPs) have been constructed around world. The unclear feedback loops of water supply-hydropower generation-environmental conservation (SHE) nexus with IWDPs increase the uncertainty in the rational scheduling of water resources for the water receiving and water donation areas. To address the different impacts of IWDPs on the dynamic SHE nexus and explore synergies, a framework is proposed to identify these impacts across the multiple temporal and spatial scales in a reservoirs group. The proposed approach was applied to the Hanjiang River Basin (HRB) in China as a case study. Runoff series from the HRB at multiple temporal and spatial scales were provided through the Variable Infiltration Capacity hydrological model. Multi-level ecological flows were determined by the Modified Tennant Method Based on Multilevel Habitat Conditions method. 30 scenarios were set and modeled in a multisource input-output reservoir generalization model. Differences between scenarios were quantified with a response ratio indicator. The results indicate that without IWDPs there are negative feedbacks between water supply (S) and hydropower generation (H), between S and environmental conservation (E) while positive feedbacks between H and E. The negative feedbacks of S on H and the positive feedbacks of E on H are weakened or even broken in abundant water periods. With IWDPs, the water donation basins experience strengthened feedback loops, while water receiving basins experience weakened feedbacks. Feedback loops exhibit intrinsic similarity and stability across different time scales. Feedbacks in reservoirs with a regulation function remain stable under the varying inflow conditions and feedbacks for downstream reservoirs are influenced by their upstream reservoirs, especially in low flow periods. Simply increasing water receiving cannot resolve inherent SHE conflicts because of the persistent feedback polarity with IWDPs, and adaptive allocation rules are needed that account for these stable feedback patterns. The proposed approach can help quantify the impacts of IWDPs on SHE nexus and contribute to the sustainable development of SHE nexus.

1 Introduction

Water resources are fundamental to life, as well as economic and social development (MacGREGOR, 1963). Water supply, hydropower generation, and environmental conservation constitute the three primary components of water resource utilization in a basin (Chung et al., 2021), delivering substantial economic, social, and ecological benefits to both humanity and nature. However, over the past 70 years, global water resources have been rapidly consumed and utilized, due to the increasing human demand and climate change, leading to complex supply-demand conflicts (Tauro, 2021; Wang et al., 2024). Water supply, hydropower generation, and environmental conservation compete, coordinate, and are interdependent with each other, and

intricate relationships can be found among them (Stickler et al., 2013). The interdependencies among these water supply (S), hydropower generation (H), and environmental conservation (E) components are referred to as an SHE nexus (Endo et al., 2017; FAO., 2014; Sanders and Webber, 2012). Identifying the SHE nexus can elucidate the trajectory of water resources system evolution under various water resource management strategies, balance the relationships among water users, and promote sustainable resource use and ecological health (Mansour et al., 2024; Zhao et al., 2021).

The current studies on the nexus primarily focus on the three fundamental resources: water, energy, and food (Conway et al., 2015; Quer et al., 2024; Wang et al., 2023). The SHE nexus refines the water-energy-food nexus and emphasizes basin-scale water resource management (Chen et al., 2020). Most of the studies on SHE nexus take reservoirs as nodes, and primarily focus on multi-objective optimization of basin-wide water resource scheduling (Khalkhali et al., 2018; Qiu et al., 2021; Tang et al., 2024). Through game-theoretical analyses among components, they aim to identify feedback between their paired components. From the perspective of reservoir nodes under scrutiny, current research primarily focuses on single reservoirs (Wu et al., 2021), virtual reservoirs (Chen et al., 2020), and cases of two connected reservoirs (Khalkhali et al., 2018). To optimize the allocation of basin-scale water resources, the deployment of cascade reservoir systems has increased significantly (Liu et al., 2022), wherein multiple reservoirs with different priority functions are strategically interconnected through series-parallel hydraulic linkages. These reservoirs form what we call a reservoirs group. A reservoirs group collaboratively manages the basin's water resource development and utilization. The different priority functions of reservoirs lead to different SHE Nexus. It is conducive to deciphering the nexus of and the directional changes within the SHE system, that the reservoirs are located in different locations within a basin, prioritizing different objective functions. Moreover, quantification of the E component often relies on the Tennant method (Tennant, 1976; Tharme, 2003) to estimate ecological flows (EFs) while neglects the temporal and spatial variations. Some of the E components only contain urban and rural ecological water use, and neglects the in-stream EFs (Chen et al., 2020). There is often not a straightforward positive or negative correlation between water supply, hydropower generation, and environmental conservation components (Zitzler, 2007). The feedback loops among components can dynamically change when observed across different temporal and spatial scales (Keyhanpour et al., 2021). The components S, H, and E interact dynamically over time and space (Dong et al., 2019), inevitably leading to changes in the feedback loops of SHE nexus. However, studies on these changes in the SHE nexus are relatively scarce. Identifying synergy within competitive loops or competition within synergetic loops across various time-space scales enhances understanding of the dynamic changes in the SHE nexus. And it also provides strategies for dealing with competition among different users in actual water management. Therefore, it is critical to investigate the bidirectional and dynamic feedback loops of the SHE nexus across multiple temporal and spatial scales.

Due to frequent extreme events and intensive human activities, the spatial and temporal distribution of water resources exhibit more and more unevenness (Wang et al., 2024). The imbalance of water supply-demand has widely spread all over the world. Inter-basin water diversion projects (IWDPs), also commonly referred to as inter-basin water transfers (IBWTs, Dong et al., 2023; Sheng et al., 2024), have been widely implemented to solve the imbalance (Siddik et al., 2023) through transferring water resources from water-rich areas (i.e., water donating area) to water-deficient regions (i.e., water receiving area) through channels and other hydraulic engineering works. The initiatives of the IWDPs seek to alleviate the imbalance among different basins but also result in notable changes in the water resource systems in both the source and receiving areas (Long et al., 2020). Many studies have extensively examined the receiving effects of IWDPs on the three components (Tang et al., 2022; Tao et al., 2008; Wei et al., 2024), as well as on the comprehensive evaluation of water resource systems (Kattel et al., 2019; Zhao et al., 2017) and multi-factor risk assessment of water donating areas (Bai et al., 2023; Mu et al., 2024; Yang et al., 2023) at different temporal and spatial scales. It was found that the dynamic planning and operation of IWDPs exert significant external impacts on the SHE system, inevitably leading to the system's "change-response-reconstitute" process. These impacts changed the

feedback loops among components of the SHE system. Additionally, studies have primarily emphasized single water donating or receiving impacts, overlooking the different impacts of IWDPs on the SHE nexus and the comprehensive effects of multi-IWDPs. Water management regulations with IWDPs have become one of the focuses in the SHE nexus (Mok et al., 2015). The current studies on this issue have primarily examined the optimal water allocation methods for negotiations among water users in donating and receiving areas. They often employ case study approaches (e.g., interviews, field studies, policy reviews, and surveys) (Zhao et al., 2017) or inter-basin water resource allocation models (Ouyang et al., 2020; Wu et al., 2022). However, most of these studies have still oversimplified the interactions among these three components as only competitive (Yan et al., 2020). Identifying the changes in the feedback loops with IWDPs and synergies following the feedback loop changes are crucial steps in improving water dispatching and management in both donating and receiving areas.

One of the aims of this study is to identify the different impacts of IWDPs across multiple temporal and spatial scales on the dynamic SHE nexus in a reservoirs group with different priority functions. Another is to explore a way to search synergies in the feedback loops of the SHE nexus. The research framework and methods are presented in Section 2, and our case study to verify the proposed framework is detailed in Section 3. Section 4 covers the results and Section 5 provides a comprehensive discussion. Conclusions are drawn in Section 6. All abbreviations used in this paper are listed in Supplementary material Table S6.

2 Methodology

2.1 Research framework

To address the impacts of IWDPs across the multiple temporal and spatial scales on the dynamic SHE nexus, multiple temporal and spatial scale runoff simulations from the water donating basins are provided through a distributed hydrological model. Multi-level ecological flows and their corresponding multi-level ecological flow standards are also determined according to an available method with spatial-temporal variability. To facilitate the identification of the impacts of IWDPs on SHE nexus, scenario experiments are set by "with/without IWDPs". In order to take the different clusters of IWDPs into account, scenario experiments are classified by the impacts of IWDPs on water donation area, on water receiving area or on an area with both water donation and water receiving if there are IWDPs. To evaluate the feedback loops of the SHE nexus, the priority order of S, H, and E are iteratively set in all reservoir nodes. We set different types of the highest priority in S, H, and E and take the standard scheduling rules as reference scenarios. All scenarios are modelled in a multisource input-output reservoir generalization model, and differences between scenarios are quantified with a response ratio indicator. And the feedback loops with the different impacts of IWDPs are identified through a response ratio indicator. To explore the synergies, a positive mutation in a response ratio across time-space is found between pairwise components of SHE. This framework can be applied globally to identify the feedbacks of the SHE nexus in basins with IWDPs. Thus, our research framework is illustrated in Figure 1. The Nexus I-III in Figure 1 are defined as the nexus with IWDPs, the nexus without IWDPs and the nexus with the different clusters of IWDPs.
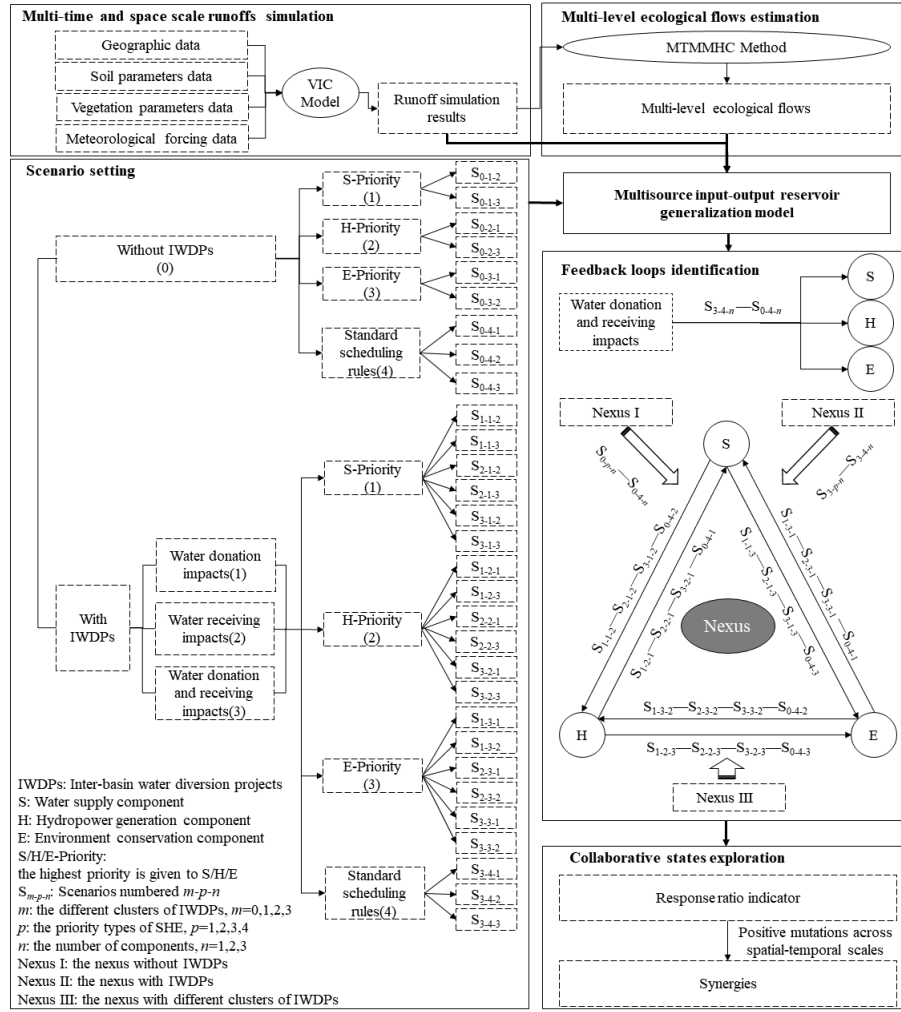
Figure 1. Framework to identify the impacts of different IWDPs on the feedback loops of SHE nexus.

2.2 The Variable Infiltration Capacity hydrological model

To simulate runoff results at multiple temporal and spatial scales, the Variable Infiltration Capacity (VIC) hydrological model is selected. The VIC model offers significant advantages in multiple temporal and spatial scale runoff simulations. It is a large-scale distributed hydrological model based on the spatial distribution grid of Soil Vegetation Atmospheric Transfer Schemes (SVATS) (Liang, et al., 1994), making it highly adaptable to studies at different spatial scales and supporting a wide range of input data types. The VIC model can simulate hydrological processes at various time scales, from hourly to annual, catering to different research needs. It excelled at simulating both the energy balance and water balance between the land and atmosphere, thereby addressing the oversight of energy processes in traditional hydrological models. The VIC model has been widely applied in runoff simulations across various basins worldwide, consistently yielding outstanding results (Wang et al., 2012; Yeste et al., 2024; Su et al., 2024). There are five steps to construct a VIC model (Koohi et al., 2022): ① collect and organize data; ② preprocesses of the VIC model; ③ construct VIC model of the selected basin; ④ run the catchment module; ⑤ parameter calibration and validation. During the calibration process, important parameters highlighted in Table 1 are automatically calibrated using MATLAB to achieve the optimal parameter combination.

Table 1. Characteristics of parameters for model optimization (Gou et al., 2020).

No.	Parameter	Brief description	Unit	Range
1	B	The power of the equation for the variable infiltration curve	/	[0,0.4]
2	D_{smax}	The maximum baseflow velocity	mm/day	[0,30]

3	D_s	The ratio of the nonlinear baseflow to D_{smax}	/	[0,1]
4	W_s	The ratio of nonlinear baseflow to saturated soil moisture content when it occurs	/	[0,1]
5	d_1	Thickness of the top layer of soil	m	[0.05,0.1]
6	d_2	Thickness of the second layer of soil	m	[0,2]
7	d_3	Thickness of the third layer of soil	m	[0,2]

125

In order to verify the accuracy of the runoff simulation results, the simulations need to be compared with the observations. Three widely used quantitative indices of numerical differences are selected, and they are the Nash-Sutcliffe efficiency coefficient (*NSE*, Nash and Sutcliffe, 1970), Coefficient of determination (*R^2*, Rousseeuw and Leroy, 1987), and Percent bias (*PBIAS*, Bland and Altman, 1986):

130
$$NSE = 1 - \frac{\sum_{t=1}^{T}\left(Q_t^o - Q_t^s\right)^2}{\sum_{t=1}^{T}\left(Q_t^o - \overline{Q^o}\right)^2} \tag{1}$$

$$R^2 = \frac{\left[\sum_{t=1}^{T}\left(Q_t^o - \overline{Q^o}\right)\left(Q_t^s - \overline{Q^s}\right)\right]^2}{\sum_{t=1}^{T}\left(Q_t^o - \overline{Q^o}\right)^2 \sum_{t=1}^{T}\left(Q_t^s - \overline{Q^s}\right)^2} \tag{2}$$

$$PBIAS = \frac{\sum_{t=1}^{T}\left(Q_t^o - Q_t^s\right) \times 100}{\sum_{t=1}^{T} Q_t^o} \tag{3}$$

where, Q_t^o and Q_t^s are the observed and simulated runoff results at *t*th month, m^3/s. $\overline{Q^o}$ and $\overline{Q^s}$ are the average of the observed and simulated runoff results over the whole period *T*, m^3/s. $NSE \in (-\infty, 1]$, the closer *NSE* is to 1, the better the

135 simulations are. The *NSE* of the simulations greater than 0.5 is acceptable. $R^2 \in [0,1]$, *R^2* approaching 1 means the simulations are equal to the observations. *PBIAS* is utilized to quantify the cumulative deviation between the simulations and observations. *PBIAS* larger than 0 meant that the simulations are generally small, and vice versa, the simulations are generally larger. When $|PBIAS| < 25\%$, the runoff simulation results are acceptable.

After getting the acceptable runoff simulation results at the selected hydrological stations, the runoff to reservoirs and the

140 interval runoff of each pair of reservoirs are estimated according to the catchment area ratio of each reservoir with its upstream and downstream hydrological stations. The calculation formulas are as follows:

$$Q_{i,t}^s = \begin{cases} \dfrac{Q_{d,1,t}^s \times A_1}{A_{d,1}}, i = 1 \\[2ex] Q_{u,i,t}^s + \dfrac{\left(Q_{d,i,t}^s - Q_{u,i,t}^s\right) \times \left(A_i - A_{u,i}\right)}{\left(A_{d,i} - A_i\right)}, i > 1 \end{cases} \tag{4}$$

$$\Delta Q_{i,t} = Q_{i,t}^s - Q_{i-1,t}^s, i > 1 \tag{5}$$

where $Q_{i,t}^s$ is the runoff to the *i*th reservoir at *t*th period, m^3/s; $Q_{u,i,t}^s$ and $Q_{d,i,t}^s$ are the simulation runoff results of the upstream

and downstream hydrological stations of the ith reservoir at tth period, m³/s; A_i is the catchment area of ith reservoir, m²; $A_{u,i}$

and $A_{d,i}$ are the catchment areas of the upstream and downstream hydrological stations, m². $\Delta Q_{i,t}$ is the interval runoff of the

ith reservoir at tth period, m³/s.

The inflow to the ith reservoir is the sum of the discharge from the $(i-1)$th reservoir and the interval runoff. The calculation

formulas are as follows:

$$Q_{i,t} = \begin{cases} Q^s_{1,t}, i = 1 \\ Q_{\mathrm{out},i-1,t} + \Delta Q_{i,t}, i > 1 \end{cases} \tag{6}$$

where $Q_{i,t}$ is the inflow to the ith reservoir at tth period, m³/s; $Q_{\mathrm{out},i-1,t}$ is the water release from the $(i-1)$ th reservoir in period

t, m³/s."

2.3 The Modified Tennant Method Based on Multilevel Habitat Conditions method

In order to establish a multi-level ecological flow standard to aid in evaluating river ecological health, the multi-level ecological flows are estimated by the MTMMHC method. There are over 200 methods for ecological flows (EFs) estimation worldwide, typically categorized into four types: hydrological, hydraulic, habitat simulation, and holistic methods (Tharme, 2003). The Tennant method, which determines EFs based on predetermined percentages of average annual flow, is the most widely used hydrological method (Tharme, 2003). The MTMMHC method (Li and Kang, 2014) modifies the Tennant method based on three parameters: average periodic flow, water period, and percentage. It can solve four key problems that exist in the current ecological flow standards: spatial transferability, monthly variability, inter-annual variability and scalability (Li, et al., 2015). Indeed, the MTMMHC method can avoid the impacts of extreme inter-annual flow events and uneven intra-annual distribution. This enables the calculation of different guarantee rates for various river sections, water years (e.g., wet, normal, and dry years), and months. It reflects the temporal and spatial variability of EFs and provides comprehensive and reasonable multi-level ecological flows standards. The steps of the MTMMHC method are as follows.

① The year groups are divided into wet years (precipitation below the 25th percentile, P<25 %), normal years (25 %≤P≤75 %), and dry years(P>75 %) firstly. Then, a flow duration curve (FDC, Franchini et al., 2011) is constructed using the total-period method based on daily average flows simulated from 1976-2020 by the VIC model. Finally, the average of flows corresponding to the 90th and 95th percentiles of the FDC ($Q_{(90)xy}$ and $Q_{(95)xy}$, m³/s) for the yth month of the xth year is taken as the Minimum Ecological Flow (MEF_{xy}, m³/s). The formula is as follows:

$$MEF_{xy} = \frac{Q_{(90)xy} + Q_{(95)xy}}{2} \tag{7}$$

② The MTMMHC method takes 50 % flow of the FDC ($Q_{(50)xy}$, m³/s) for the yth month of the xth year as the maximum of the Optimum Ecological Flow ($OEF_{xy\,(max)}$, m³/s). According to the Tennant method, the EFs are assumed to be ten levels, and the minimum of the Optimum Ecological Flow ($OEF_{xy\,(min)}$, m³/s) is set as level six, and the formulas are as follows:

$$OEF_{xy(max)} = Q_{(50)xy} \tag{8}$$

$$OEF_{xy(min)} = \frac{5Q_{(50)xy} + 4MEF_{xy}}{9} \tag{9}$$

③ The MTMMHC method computes EFs at all levels using the arithmetic difference between MEF_{xy} and $OEF_{xy\,(min)}$. The MTMMHC method eliminates the classification of $OEF_{xy\,(min)}$—$OEF_{xy\,(max)}$, resulting in the grading number of EFs to be $R+1$.

The mode of all the grading number of selected stations is taken as the grading number R:

$$R = \text{Mode}\left(\text{Average}\left(m_{xy}\right)\right) \tag{10}$$

$$m_{xy} = \text{Round}\left(\frac{5}{9} \times \frac{Q_{(50)xy} - MEF_{xy}}{0.1 \times Q_{(50)xy}}\right) + 1 \tag{11}$$

where, m_{xy} is the grading number between MEF_{xy} and $OEF_{xy(min)}$ in the yth month and xth year; Mode($\cdot$), Average($\cdot$), and Round($\cdot$) are the functions which return the most frequently occurred number in Average (m_{xy}), the average of m_{xy}, and the nearest integer.

④ Based on the hierarchical idea of arithmetic progression, a range of EFs criteria can be defined as follows:

$$EF_{xy(r)} = MEF_{xy} + \frac{5}{9} \times \frac{r-1}{R-1}\pi\left(Q_{(50)xy} - MEF_{xy}\right) \tag{12}$$

where, $EF_{xy(r)}$ is the rth level ecological flow in the yth month of the xth year, m³/s.

2.4 The Log Response Ratio method for identifying feedback loops

2.4.1 Water supply, hydropower generation and environment conservation indexes

To evaluate the state of S, H, and E, the water supply volume, hydropower generation, and ecological flow satisfaction rate as indexes of the three components are set. The formulas are as follows.

① Regional water supply volume:

$$V_{s,i,t} = Q_{s,i,t} \times \Delta t = V_{i,t} - V_{i,t+1} + \left(Q_{out,i-1,t} + \Delta Q_{i,t} + Q_{re,i,t} - Q_{out,i,t} - Q_{do,i,t}\right)\Delta t - I_{i,t} \tag{13}$$

where, $V_{s,i,t}$ is the regional water supply volume, m³; $Q_{s,i,t}$ is the regional water supply flow, m³/s; Δt is the time interval, s; $V_{i,t}$ and $V_{i,t+1}$ are the storage of the ith reservoir in period t and $t+1$, m³; $Q_{out,i-1,t}$ is the water release from the (i-1)th reservoir in period t, m³/s; $\Delta Q_{i,t}$ is the flow of the intervening basin between the (i–1) th and ith reservoirs in period t, m³/s. $Q_{re,i,t}$ is the water receiving from IWDPs, m³/s, and $Q_{do,i,t}$ is the water donation for IWDPs, m³/s. $I_{i,t}$ is the sum of evaporation and seepage losses from the reservoir in period t, m³, respectively.

② Hydropower generation：

$$E_{i,t} = \sum_{t=1}^{T} N_{i,t}\Delta t \qquad N_{i,t} = K_i Q_{e,i,t} H_{i,t} \qquad K_i = \eta_i g \rho \tag{14}$$

where, $E_{i,t}$ is the hydropower generation of the ith reservoir, kW·h; $N_{i,t}$ is the output of the ith reservoir in the tth period, kW; K_i is the comprehensive hydropower coefficient of the ith reservoir, kg/(s²·m²); η_i is the hydropower generation efficiency; g is the gravitational acceleration, m/s²; ρ is the density of water, kg/m³; $Q_{e,i,t}$ and $H_{i,t}$ are the release discharge for hydropower generation, m³/s, and the average hydropower head of the ith reservoir in period t, m, respectively.

③ Ecological flow satisfaction rate is used to evaluate the satisfaction of intra-river flow to multi-level ecological flow standard. It is quantified through the segmented linear affiliation function:

$$EFSR_{xy} = \begin{cases} 0 & EF_{xy} \leq \dfrac{E_{xy(1)}}{2} \\[2ex] \dfrac{1}{R+1}\left(\dfrac{EF_{xy} - \dfrac{E_{xy(1)}}{2}}{E_{xy(1)} - \dfrac{E_{xy(1)}}{2}}\right) & \dfrac{E_{xy(1)}}{2} < EF_{xy} \leq E_{xy(1)} \\[2ex] \dfrac{1}{R+1} + \dfrac{1}{R+1}\left(\dfrac{EF_{xy} - E_{xy(1)}}{E_{xy(2)} - E_{xy(1)}}\right) & E_{xy(1)} < EF_{xy} \leq E_{xy(2)} \\[2ex] \dfrac{2}{R+1} + \dfrac{1}{R+1}\left(\dfrac{EF_{xy} - E_{xy(2)}}{E_{xy(3)} - E_{xy(1)}}\right) & E_{xy(2)} < EF_{xy} \leq E_{xy(3)} \\[2ex] \cdots & \cdots \\[2ex] \dfrac{R-1}{R+1} + \dfrac{1}{R+1}\left(\dfrac{EF_{xy} - E_{xy(R-1)}}{E_{xy(R)} - E_{xy(R-1)}}\right) & E_{xy(R-1)} < EF_{xy} \leq E_{xy(R)} \\[2ex] \dfrac{R}{R+1} + \dfrac{1}{R}\left(\dfrac{EF_{xy} - E_{xy(R-1)}}{E_{xy(R)} - E_{xy(R-1)}}\right) & E_{xy(R)} < EF_{xy} \leq E_{xy(R+1)} \\[2ex] 1 & E_{xy(R+1)} < EF_{xy} \end{cases} \tag{15}$$

where, $EFSR_{xy} \in [0,1]$, is the ecological flow satisfaction rate in the yth month of the xth year. $E_{xy(1)}$, $E_{xy(R)}$ and $E_{xy(R+1)}$ are

MEF_{xy}, $OEF_{xy(\min)}$ and $OEF_{xy(\max)}$, respectively.

2.4.2 The Multisource Input-Output Reservoir Generalization (MIORG) model for a reservoirs group

Reservoirs can determine S, H, and E according to their scheduling rules. To quantify the differences of indexes with different impacts of IWDPs in reservoir nodes, MIORG models for reservoirs group are developed. For a single reservoir, the inputs generally refer to the inflow from the upstream and water receiving from IWDPs. The outputs from this MIORG model refer to regional water supply (i.e., domestic, industrial, and ecological water supply), water donation for IWDPs, evaporation and seepage losses, water release from the reservoir. The multisource input-output to a single reservoir is shown in Figure 2.
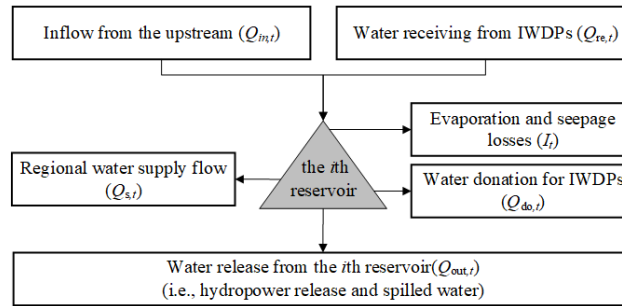
Figure 2. The multisource input-output to a single reservoir.

According to the principle of water balance, the MIORG model for a single reservoir is developed as follows:

$$V_{t+1} = V_t + \left(Q_{in,t} + Q_{re,t} - Q_{s,t} - Q_{out,t} - Q_{do,t}\right)\Delta t - I_t \tag{16}$$

For a reservoirs group, the inputs to ith reservoir can be categorized into: water release from the upstream reservoir (i.e., the (i-1) th reservoir), the flow of the intervening basin and water receiving from IWDPs. The outputs from ith reservoir in a reservoirs group are same as those from a single reservoir. The multisource input-output to ith reservoir in a reservoirs group is shown in Figure 3. The MIORG model for the ith reservoir in a reservoirs group is:

$$V_{i,\,t+1} = V_{i,\,t} + \left(Q_{\text{out},i-1,t} + \Delta Q_{i,t} + Q_{\text{re},i,t} - Q_{\text{s},i,t} - Q_{\text{out},i,t} - Q_{\text{do},i,t} \right) \Delta t - I_{i,t} \tag{17}$$
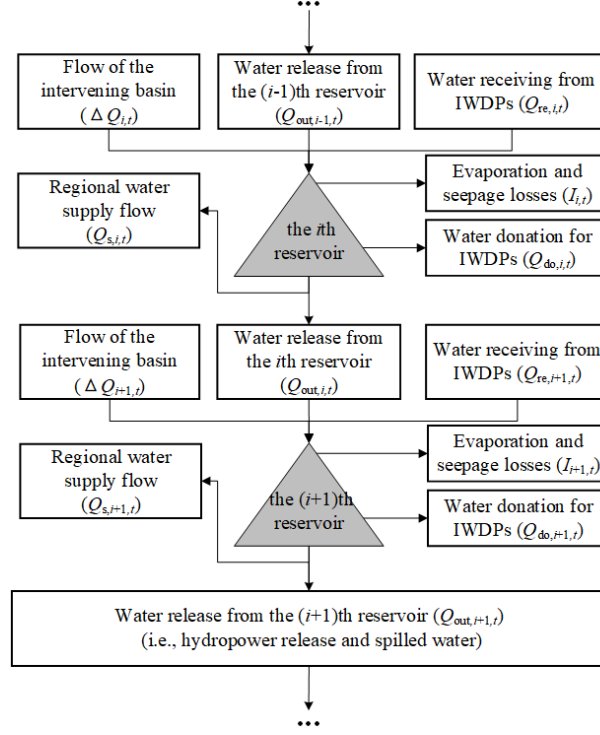
$\cdots$

Figure 3. The multisource input-output to reservoirs in a reservoirs group.

2.4.3 The Log Response Ratio method

To analyse the feedback loops in Nexus I, Nexus II and Nexus III in Figure 1, the log response ratio (*LRR*) method (Patrick et al., 2022) is used to quantify the responses of S, H, and E with different clusters of IWDPs. This method captures non-linear feedback loops within complex SHE nexus systems. The formula is as follows:

$$LRR_n = \ln\left(\frac{\left(r_{c(n)} - r_n \right) + r_n}{r_n} \right) = \ln\left(\frac{r_{c(n)}}{r_n} \right) \tag{18}$$

where LRR_n is the log response ratio of the nth component; n represents the performance evaluation component (1: water supply component; 2: hydropower generation component; 3: environmental conservation component); LRR_1 refers to the log response ratio of water supply volume between the two compared scenarios, characterizing the differences in the S component. Correspondingly, LRR_2 and LRR_3 represent the differences in the H and E components between two compared scenarios, respectively. r_n is the value of regional water supply volume or hydropower generation or ecological flow satisfaction rate in the baseline scenario. $r_{c(n)}$ is the value of the index in the compared scenario. $r_{c(n)}$ and r_n are both greater than or equal to zero. The positive LRR_n indicates $r_{c(n)} > r_n$, meaning the compared scenario improves the component relative to the baseline. The negative LRR_n indicates $r_{c(n)} < r_n$, meaning the compared scenario worsens the component relative to the baseline. The absolute value of LRR_n reflects the degree of change on a logarithmic scale. The larger the absolute value of LRR_n, the more substantial the improvement (if positive) or worsening (if negative) is when measured logarithmically.

2.5 Scenario setting

To identify the impacts of different clusters of IWDPs on the SHE nexus, scenarios are set according to the following three aspects: with or without IWDPs (i.e., two types for IWDPs), different clusters of IWDPs (i.e., four clusters for the above two

types), and the priority orders of S, H, and E. As there are three components for the highest priority, six scenarios can be obtained through the combination of the three components. As all S, H, and E are determined from standard scheduling rules, there are also three types of standard scheduling rules. Combined with the types of different clusters of IWDPs, there will be a total of 30 scenarios (i.e., 4 clusters of IWDPs $\times$ 6 types for the highest priority combinations +2 types for IWDPs $\times$ 3 types for standard scheduling rules) as listed in Table 2. Specifically, to iteratively set the priority orders of S, H, and E, all three components are all in standard scheduling rules firstly. Secondly, the highest priority is set to water supply (as denoted by S-Priority), which means all reservoirs will first meet regional water demands (i.e., domestic, industrial, and ecological), with surplus water then allocated to hydropower generation and environment conservation needs. Additionally, increasing the regional water supply to 120% enhances the observability and analytical prominence of the quantitative outcomes derived from these nexus. Thirdly, hydropower generation (H-Priority) is prioritized to achieve the maximum output during the planned period. Finally, environmental conservation (E-Priority) is addressed through ensuring that the reservoir outflow meets $OEF_{xy(\max)}$. These scenarios offer flexibility in modeling SHE nexus system behavior under different conditions.

The scenarios are named in the format S_{m-p-n}, where m represents the different clusters of IWDPs (0: without IWDPs; 1: with only water donation; 2: with only water receiving; 3: with both donation and receiving), p represents the priority types of S, H, and E (1: the highest priority is water supply; 2: the highest priority is hydropower generation; 3: the highest priority is environmental conservation; 4: standard reservoir scheduling rules), and n represents the performance evaluation component (1: water supply component; 2: hydropower generation component; 3: environmental conservation component).

To analyse the feedback loops of SHE nexus without IWDPs, the differences between the S_{0-p-n} (p=1, 2, 3) and S_{0-4-n} scenarios are determined (i.e., the feedback loops of Nexus I as shown in Figure 1). To analyse the feedback loops with IWDPs (i.e., the feedback loops of Nexus II as shown in Figure 1), the differences between the S_{3-p-n} (p=1, 2, 3) and S_{3-4-n} scenarios are determined. Thus, the differences between Nexus I and Nexus II show the impacts of IWDPs on the SHE nexus. To identify the SHE nexus with different clusters of IWDPs (i.e., the feedback loops of Nexus III as shown in Figure 1.), the differences between S_{m-p-n} (m=1, 2, 3; p=1, 2, 3) and S_{0-4-n} scenarios are determined. The differences between Nexus I and Nexus III show the impacts of different IWDP clusters on the SHE nexus. S_{0-4-n} (i.e., the scenarios with standard scheduling rules without IWDPs) and S_{3-4-n} (i.e., the scenarios with standard scheduling rules with IWDPs), are the baseline scenarios for distinguishing Nexus I, Nexus III, and Nexus II. In the same way, to clarify the impacts of IWDPs on the three components, the differences between the S_{0-4-n} and S_{3-4-n} scenarios are determined.

Table 2. The scenarios to identify the impacts of different clusters of IWDPs on the SHE nexus.

Different clusters of IWDPs (m)	The priority orders of S, H, and E (p)			Scenarios
	S	H	E	
Without IWDPs	\ (0)			S_{0-4-1}
		ISQ		S_{0-4-2}
				S_{0-4-3}
		S-Priority	\	ISQ	S_{0-1-2}
		S-Priority	ISQ	\	S_{0-1-3}
		\	H-Priority	ISQ	S_{0-2-1}
		ISQ	H-Priority	\	S_{0-2-3}
		\	ISQ	E-Priority	S_{0-3-1}
		ISQ	\	E-Priority	S_{0-3-2}
With IWDPs	With water donation impacts (1)	S-Priority	\	ISQ	S_{1-1-2}
		S-Priority	ISQ	\	S_{1-1-3}
		\	H-Priority	ISQ	S_{1-2-1}

10

	ISQ	H-Priority	\	S1-2-3
	\	ISQ	E-Priority	S1-3-1
	ISQ	\	E-Priority	S1-3-2
With water receiving impacts (2)	S-Priority	\	ISQ	S2-1-2
	S-Priority	ISQ	\	S2-1-3
	\	H-Priority	ISQ	S2-2-1
	ISQ	H-Priority	\	S2-2-3
	\	ISQ	E-Priority	S2-3-1
	ISQ	\	E-Priority	S2-3-2
With water donation and receiving impacts (3)		ISQ		S3-4-1
				S3-4-2
				S3-4-3
	S-Priority	\	ISQ	S3-1-2
	S-Priority	ISQ	\	S3-1-3
	\	H-Priority	ISQ	S3-2-1
	ISQ	H-Priority	\	S3-2-3
	\	ISQ	E-Priority	S3-3-1
	ISQ	\	E-Priority	S3-3-2

* ISQ (In Status Quo) indicates that the component operates under the standard scheduling rules for reservoirs.

3 Study area and data

3.1 Overview of the study area

275 The Hanjiang River, as the largest tributary of the Changjiang River, plays an important role in China's economic development and ecological environment (Xia et al., 2020). The Hanjiang River originates from the Qinling Mountains, and it traverses Shaanxi, Hubei, and Henan before joining the Changjiang River in Wuhan. The Hanjiang River Basin (HRB) has a basin area of about 159,000 km², and has different clusters of IWDPs (Stone and Jia, 2006). In this study, we choose the Han-to-Wei Water Diversion Project (Wei et al., 2020), the Middle Route of the South-to-North Water Diversion Project (Li et al., 2016), and the

280 Northern Hubei Water Resources Allocation Project (He and X, 2020) to analyze the water donation impacts of IWDPs on the SHE nexus. The Three Gorges Reservoir to Hanjiang River (Yang et al., 2012) and the Changjiang-to-Han River Water Diversion Project (Zhang et al., 2022) are selected to discuss the water receiving impacts in HRB. All IWDPs follow its scheduling rules for donation and receiving. The HRB hosts numerous reservoirs, with a cascade of 15 reservoirs along its mainstream, starting with the Huangjinxia Reservoir. These reservoirs play significant roles in flood control, water supply,

285 hydropower generation, and ecological conservation (Liu et al., 2018). The Huangjinxia Reservoir (HJX), Ankang Reservoir (AK), Danjiangkou Reservoir (DJK), Wangfuzhou Reservoir (WFZ), and Xinglong Reservoir (XL) are chosen as research nodes due to their extensive spatial distribution and different priority orders of S, H, and E. Among them, HJX, DJK, and XL are water supply-prioritized reservoirs, while AK and WFZ are hydropower generation-prioritized reservoirs. The overview map of HRB and the sketch graphic are shown in Figures 4 and 5. The characteristic parameter values of reservoirs are listed
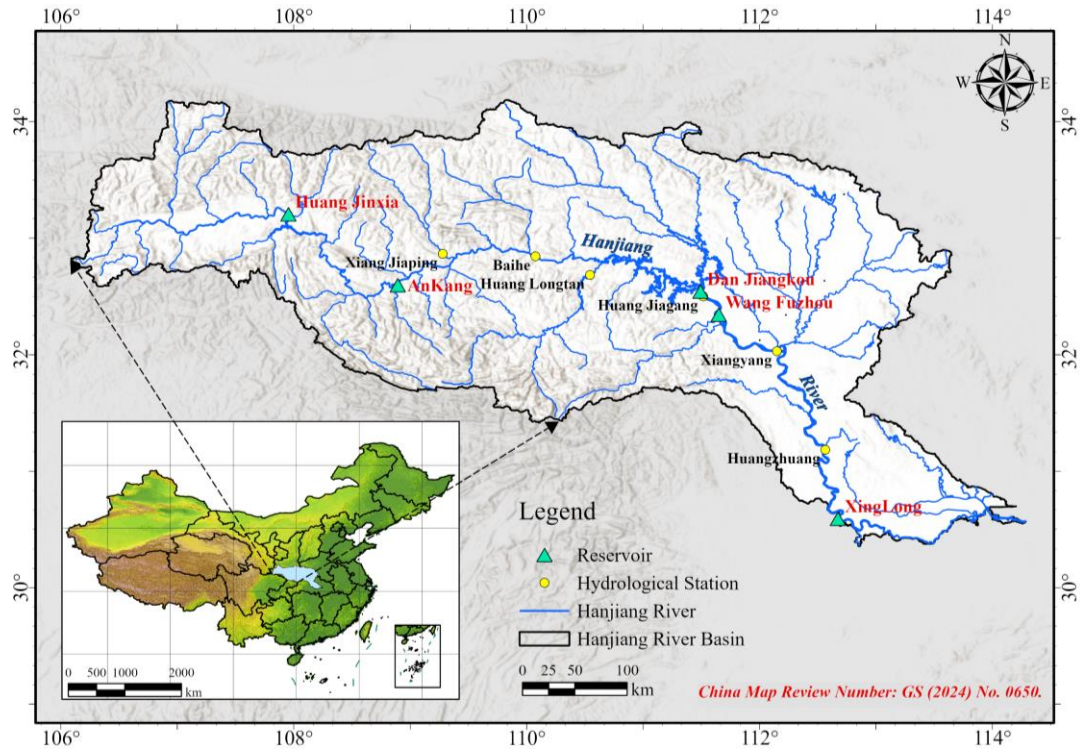
290 in Table 3.
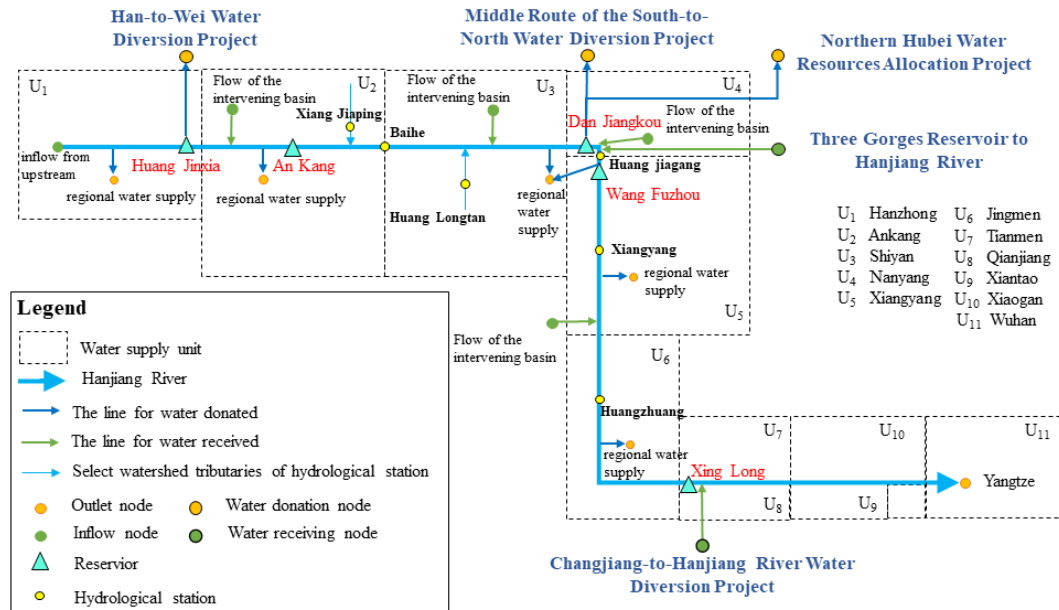
Figure 4. Overview map of the study area.

Figure 5. The sketch graphic of the Hanjiang River Basin (adapted from Zeng et al., 2023).

295   **Table 3**. List of characteristic parameter values of reservoirs.

| Characteristic parameter	Unit	Huang Jinxia	An Kang	Dan Jiangkou	Wang Fuzhou	Xing Long
Operational year	year	2023	1992	2013	2003	2013
Normal water level	m	450	330	170	86.23	36.2
Usable storage	$10^6 m^3$	92	1680	16360	149.5	24.6
Dead water level	m	440	305	150	85.48	35.7
Installed capacity	MW	135	800	900	109	40
Energy generation	billion kWh/yr	0.25	2.80	3.83	0.58	0.23
Comprehensive hydropower coefficient	$kg/(s^2 \cdot m^2)$	8.4	8.4	7.7	8.5	8.4
Regulation ability	time	Daily	Yearly	Multi-year	Daily	Daily

3.2 Data sources

Based on the availability of observed runoff data and water supply volume data in the HRB, 1972-2020 is chosen for runoff simulation, and the scenario simulation period is selected as 2006-2020. Observed runoff data was obtained from the Hydrology Bureau of the Changjiang Water Resources Commission, selecting monthly runoff data from six hydrological stations: Xiangjiaping, Baihe, Huanglongtan, Huangjiagang, Xiangyang, and Huangzhuang. Meteorological forcing data for the HRB was sourced from the National Meteorological Science Data Center (http://data.cma.cn/). 88 meteorological stations were selected for the daily precipitation, maximum and minimum temperatures, and average wind speed data from 1972 to 2020. These data were interpolated onto a 5-arc-minute orthogonal grid using the Inverse Distance Weighting method. Digital Elevation Model (DEM) data, with a spatial resolution of 90 meters, was provided by the Geospatial Data Cloud website (http://www.gscloud.cn/). Vegetation parameters data was sourced from the global vegetation cover classification data with 1 km resolution developed by the University of Maryland (http://www.landcover.orgdatalandcover/data.shtml). Soil parameters data was sourced from the Cold and Arid Regions Science Data Center (http://www.bdc.ac.cn/portal/) and utilizes the Harmonized World Soil Database (HWSD) created by the Food and Agriculture Organization (FAO) and Institute of Internal Auditors South Africa (IIASA), at 5 arc-minute resolution. The relevant physical parameters of soils divided into 14 types including bare soils, were estimated using the Soil-Water Characteristics (SWCT) module in the SPAW software. Reservoir characteristic parameters were primarily sourced from the official websites, reservoir design reports, and related literatures. The water supply volume data was obtained from the "Water Resources Bulletin" of cities in HRB from 2006 to 2020. Based on the water supply data from administrative regions, the water supply volume for the study area is calculated through ArcGIS.

4 Results

4.1 Calibration and verification of VIC model

The HRB was discretized into 2103 grids of 5-arc minutes. Inputting meteorological forcing, soil parameter, and vegetation parameter data for each grid, runoff was simulated. The model warm-up period was 1972-1975, its calibration from 1976 to 2005, the validation was from 2006 to 2013, while runoff from 2014 to 2020 was simulated for its post-validation. All the results are shown in Figure 6. It can be found that the accuracies of the simulations at all hydrological stations are acceptable, and superior performances were found in the upstream part of HRB. For instance, *NSE* for calibration and validation were 0.90 and 0.77, with corresponding *R²* of 0.91 and 0.87 at BH. Due to the intense human activity impacts in mid–lower reaches of the HRB, the performance was poorer at HJG while their *NSE* values still exceeded 0.60 *PBIAS* for all these six stations during calibration and validation periods ranged within [-5 %, 11 %], which indicates satisfactory agreement.
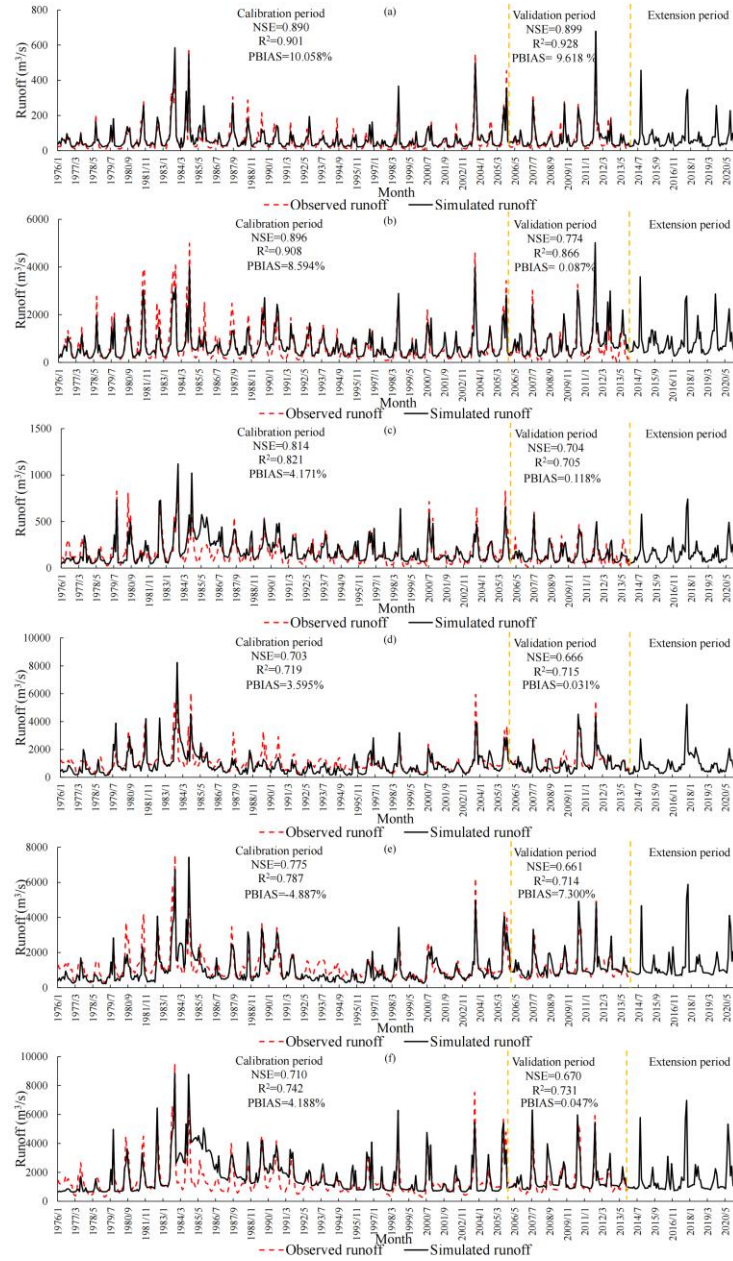
Figure 6. Calibration and validation results of simulation at hydrological stations: (a)Xiangjiangping, (b) Baihe, (c) Huanglongtan, (d) Huangjiagang, (e) Xiangyang, (f) Huangzhuang.

4.2 Multi-level ecological flows classification and calculation results

The multi-level ecological flows at HJX, AK, DJK, WFZ, and XL reservoir dam sites for each month were determined through the MTMMHC method. Their EFs are categorized into four levels: *MEF*, EF_2, OEF_{min} and OEF_{max}. The results at XL reservoir dam site from the MTMMHC method are presented in Table 4. Their Efs for wet, normal, and dry years show decreasing trends, with higher values during the flood season. Its peak ecological flow occurs in August during wet years while in July during both normal and dry years. All the peak EFs for the other four sites occur between July and September. The peak EF for HJX and AK reservoir dam sites during wet, normal, and dry years occur between July and August. The peak values for DJK and WFZ are dispersed, and they are found in September, August, and July. The EFs at the five reservoir dam sites from June to September are significantly higher than those in other months. These EFs for wet, normal, and dry years are similar to the related ecological flow quantification results in HRB (Zhang, et al., 2022, Li and Kang, 2014).

Table 4. Multi-level ecological flows resulted from MTMMHC method.

Site	Month	Wet year				Normal year				Dry year			
		MEF (m³/s)	EF_2 (m³/s)	OEF_{min} (m³/s)	OEF_{max} (m³/s)	MEF (m³/s)	EF_2 (m³/s)	OEF_{min} (m³/s)	OEF_{max} (m³/s)	MEF (m³/s)	EF_2 (m³/s)	OEF_{min} (m³/s)	OEF_{max} (m³/s)
	Jan	1197	1476	1550	1668	825	849	872	910	664	666	668	670
	Feb	1265	1467	1539	1656	836	863	890	933	675	678	681	686
	Mar	1268	1486	1569	1702	842	869	896	938	685	690	696	705
	Apr	1249	1329	1426	1581	868	892	916	955	691	698	704	714
XL dam site	May	1273	1675	1822	2058	861	887	912	953	705	714	723	738
	Jun	1653	1681	1877	2192	877	916	955	1017	763	786	809	846
	Jul	1818	2629	2987	3560	1288	1430	1572	1799	875	921	968	1043
	Aug	1885	2522	2849	3372	1266	1401	1537	1753	811	845	879	933
	Sep	1465	2822	3225	3869	1174	1279	1384	1553	834	879	924	997
	Oct	1368	2276	2611	3148	978	1036	1094	1186	733	752	772	802
	Nov	1315	1586	1748	2007	897	932	966	1022	691	697	704	714
	Dec	1194	1471	1549	1675	845	873	900	944	680	686	691	700

340

4.3 Responses of indexes in feedback loops with different clusters of IWDPs in a reservoirs group

4.3.1 Responses of indexes in feedback loops without and with IWDPs

To analyse the feedback loops of SHE nexus without (i.e., $S_{0\text{-}p\text{-}n}$ and $S_{0\text{-}4\text{-}n}$) and with IWDPs (i.e., $S_{3\text{-}p\text{-}n}$ and $S_{3\text{-}4\text{-}n}$) across the multiple temporal (i.e., monthly, seasonal and annual) and spatial (i.e., five reservoirs) scales, the differences of indexes (i.e.,

345   LRR_1, LRR_2, LRR_3 for log response ratio of the S, H, and E component) between $S_{0\text{-}p\text{-}n}$ and $S_{0\text{-}4\text{-}n}$ or between $S_{3\text{-}p\text{-}n}$ and $S_{3\text{-}4\text{-}n}$ are determined at the time scales in a reservoirs group. Monthly differences are presented in Figures 7 and 8, while the seasonal results are shown in Figure 9. Corresponding annual-scale results can be found in Supplementary material Tables S1 and S2.

If there was no IWDPs and S-Priority was set, both the mean values of LRR_2 and of LRR_3 in five reservoirs remain below 0 as shown in Figure 7 (a). As there are a large number of negative values of LRR_2 in all reservoirs with S-Priority as shown in

350   Figure 7 (a-1), the hydropower generation is found to be reduced in most months. However, there are still some positive values of LRR_2 in reservoirs. XL reservoir shows a higher occurrence of positive values of LRR_2 when there is abundant water such as July in 2007 and September in 2017. As shown in Figure 7 (a-2), all five reservoirs exhibit a negative LRR_3 in all months. The value of LRR_3 for the DJK reservoir is closest to 0. The smallest mean values of LRR_3 for the XL and AK reservoirs are -0.61 and -0.54, respectively. The reduction of ecological flow satisfaction rates for DJK is smaller than those for other reservoirs

355   due to its effective regulation. The values of ecological flow satisfaction rates for XL and AK significantly decrease due to their greater reductions of ecological flow and their higher ecological flow standards at the two reservoirs dam sites. The extreme values (e.g., lower than 90 % months values) of LRR_3 for HJX, AK, WFZ, and XL reservoirs occur in the higher water supply demand months such as June to September of each year. There are also differences between the results of LRR_2 and LRR_3, the range of LRR_3 value is wider, while its of LRR_2 is relatively concentrated and closer to 0.

360   If there was no IWDPs and H-Priority was set, the values of LRR_1 for all five reservoirs are less than zero in most months, and the mean values of LRR_3 exceed zero as shown in Figure 7 (b). The water supply for HJX, DJK, and XL is significantly decreased, while the water supply for AK and WFZ has slight reductions as shown in Figure 7 (b-1). There are two positive values of LRR_1 for DJK reservoir occurring in January 2010 and in July 2011. In January 2010, higher water storage resulting

from H-Priority increases water availability. With H-Priority, reservoirs with regulating capacity will store more water, leading to increased generation flow during dry periods (Zhang et al., 2014). While in July 2011, an increase in the discharge flow from the upstream reservoir increased the water supply. As shown in Figure 7 (b-2), the values of ecological flow satisfaction rates for HJX reservoir significantly increase. DJK and its downstream reservoirs have negative values of LRR_3 in abundant water months because of the increased storage capacity and the reduced inflow into DJK. The water resource allocation of DJK affects the SHE system of downstream reservoirs. There are also differences between the results of LRR_1 and LRR_3, the values of LRR_3 are relatively closer to 0 than those of LRR_1. The feedbacks on S are more pronounced than on E. The extreme values of LRR_1 and LRR_3 are always found in months with small water flow in river but with high-water supply demand.

If there was no IWDP and E-Priority was set, the mean values of LRR_1 for HJX, DJK, and XL reservoirs are negative as shown in Figure 7 (c-1). However, the values of LRR_1 for AK and WFZ are almost zero because their increased discharge water from upstream are prioritized to be released for hydropower generation, and no excess is for water supply. Thus, prioritizing E has less impact on S for reservoirs due to the main function of hydropower generation. DJK and XL exhibit some positive values of LRR_1 because of increased inflows from upstream. Therefore, the increased inflow to upstream reservoirs alleviates the negative feedbacks of E on S in downstream reservoirs. As shown in Figure 7 (c-2), the mean values of LRR_2 for HJX, AK, DJK, and WFZ reservoirs are positive but close to zero. While XL has a small negative mean value of LRR_2, it experiences greater decreases in hydropower generation primarily due to its smaller installed capacity (Zhang, 2008). Negative values of LRR_2 can be found in abundant water months. The ranges of LRR_1 and LRR_2 are also different. The former one is wide while the other one is narrow and their values are closer to zero.

The differences between the S_{3-p-n} and S_{3-4-n} scenarios were determined to analyse the feedback loops with IWDPs as shown in Figure 8 (a), (b), and (c). It can be found that the positive or negative signs of the LRR_n values with IWDPs are consistent with those without IWDPs. If there are IWDPs and S-Priority was set, the mean value of LRR_3 for XL shows an increase while all the values of LRR_2 and LRR_3 for other four reservoirs are lower than those without IWDPs as shown in Figure 8 (a) and Figure 7 (a). The mean values of LRR_2 with IWDPs for the five reservoirs are all negative but small, and the mean values of LRR_3 are slightly more negative. DJK reservoir get more extreme values due to the impacts of IWDPs. The values of LRR_2 with IWDPs are lower than -0.45 (i.e., the minimum value of LRR_2 without IWDPs) in 6 % of the months while the values of LRR_3 are lower than -1.40 (i.e., the minimum value of LRR_3 without IWDPs) in 8 % of the months. It is evident that IWDPs strengthen the negative feedbacks of the S component on the other two components in HJX, AK, DJK and WFZ, while IWDPs weaken negative feedbacks of S on E for XL. As shown in Figure 8 (b-1), if there were IWDPs and H-Priority was set, the mean values of LRR_1 for HJX, AK, and XL reservoirs significantly decreased, but the mean value of LRR_1 for DJK reservoir increased due to IWDPs. The differences in water supply between the S_{3-2-n} and S_{3-4-n} scenarios remain negligible despite further reductions in water supply with H-Priority. As shown in Figure 8 (b-2), the values of LRR_3 for HJX, AK, DJK, and WFZ increase further than them in Figure 7 (b-2) without IWDPs. The values of LRR_3 for XL decrease slightly due to the positive feedbacks of the H component on E and the IWDPs impacts. As shown in Figure 8 (c-1), if there were IWDPs and E-Priority was set, the mean values of LRR_1 for HJX and XL decrease. The mean values of LRR_1 for AK and WFZ remain at almost zero, while the mean value of LRR_1 for DJK increases by with IWDPs compared to without IWDPs. As shown in Figure 8 (c-2), the mean values of LRR_2 for five reservoirs increase slightly with IWDPs compared to without IWDPs. The positive feedbacks of E component on H are strengthened, while the negative feedbacks are weakened.
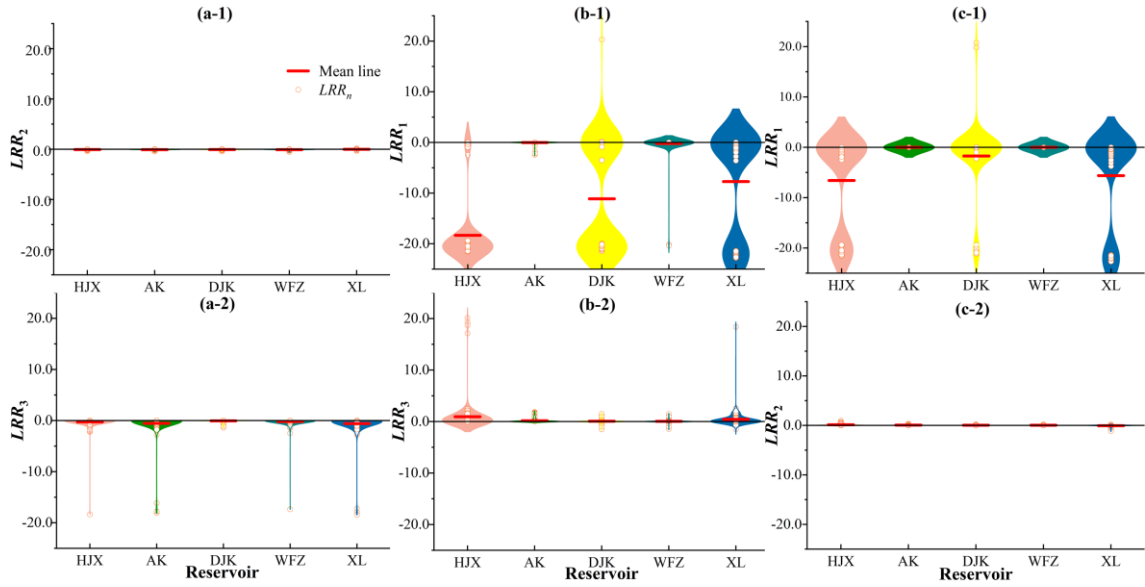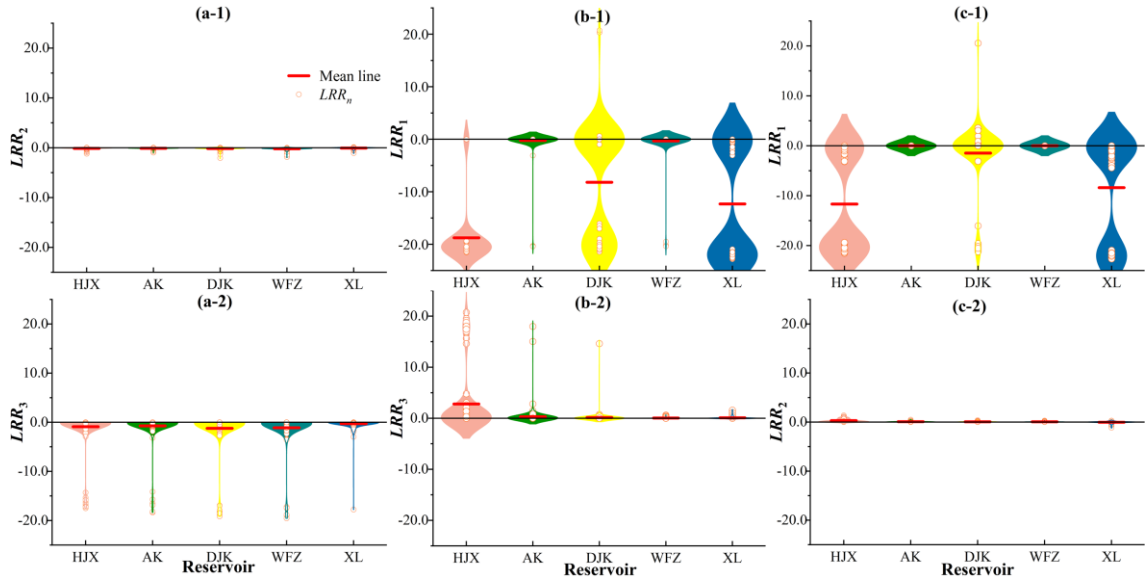
Figure 7. the differences of indexes (i.e., LRR_1, LRR_2, LRR_3 for log response ratio of the S, H, and E component) without IWDPs (i.e., between S_{0-p-n} and S_{0-4-n}) at the monthly scale: (a-1) is LRR_2 with the highest priority in S (i.e., between S_{0-1-2} and S_{0-4-2}), (a-2) is LRR_3 with the highest priority in S (i.e., between S_{0-1-3} and S_{0-4-3}), (b-1) is LRR_1 with the highest priority in H (i.e., between S_{0-2-1} and S_{0-4-1}), (b-2) is LRR_3 with the highest priority in H (i.e., between S_{0-2-3} and S_{0-4-3}), (c-1) is LRR_1 with the highest priority in E (i.e., between S_{0-3-1} and S_{0-4-1}), (c-2) is LRR_2 with the highest priority in E (i.e., between S_{0-3-2} and S_{0-4-2}).

Figure 8. the differences of indexes (i.e., LRR_1, LRR_2, LRR_3 for log response ratio of the S, H, and E component) with IWDPs (i.e., between S_{3-p-n} and S_{3-4-n}) at the monthly scale: (a-1) is LRR_2 with the highest priority in S (i.e., between S_{3-1-2} and S_{3-4-2}), (a-2) is LRR_3 with the highest priority in S (i.e., between S_{3-1-3} and S_{3-4-3}), (b-1) is LRR_1 with the highest priority in H (i.e., between S_{3-2-1} and S_{3-4-1}), (b-2) is LRR_3 with the highest priority in H (i.e., between S_{3-2-3} and S_{3-4-3}), (c-1) is LRR_1 with the highest priority in E (i.e., between S_{3-3-1} and S_{3-4-1}), (c-2) is LRR_2 with the highest priority in E (i.e., between S_{3-3-2} and S_{3-4-2}).

In this study, March, April, and May are taken as spring, June, July and August are taken as summer, September, October and November are taken as autumn, and December, January and February of the following year are taken as winter. The values of LRR_n for five reservoirs at seasonal scale are shown in Figure 9. If there was no IWDP but S-Priority was still set, positive values of LRR_2 for HJX and XL are found in summer, while all negative values of LRR_2 for other three reservoirs are found in all seasons as shown in Figure 9 (a). All values of LRR_3 for the five reservoirs are negative in all seasons. If there were IWDPs and S-Priority was set, the mean value of LRR_3 for XL increases while the values of LRR_2 and LRR_3 for other four reservoirs are less than those without IWDPs as shown in Figure 9 (b). These negative values indicate that IWDPs significantly strengthen the negative feedbacks of the S component on H and E in reservoirs and weaken negative feedback of S on E in XL. If there

17

was no IWDPs but H-Priority was set, negative values of LRR_1 and positive values of LRR_3 are found for the five reservoirs as shown in Figure 9 (c). For HJX, DJK and XL reservoirs, the negative values of LRR_1 are found in winter while zero values of LRR_1 are found in summer. The mean values of LRR_1 are close to zero in AK and WFZ reservoirs in all seasons. Positive values of LRR_3 are smaller in HJX, AK, DJK and WFZ reservoirs, while those in XL are greater in winter with a low flow. If there were IWDPs and H-Priority was set, the values of LRR_1 for all reservoirs are lower than those without IWDPs as shown in Figure 9 (d). Values of LRR_3 for HJX, AK, DJK and WFZ reservoirs are greater than those without IWDPs, while those for XL are close to zero. If there was no IWDPs and E-Priority was set, negative values of LRR_1 for HJX, DJK, WFZ and XL reservoirs can be found in almost every season, while zero values of LRR_1 for AK reservoir can be found in all seasons. As shown in Figure 9 (e), two positive values of LRR_1 for DJK are found in spring and in winter of 2007 due to the increased discharge water from AK reservoir. The positive values of LRR_2 for the five reservoirs are found in most seasons, but few negative values are found in summer. If there were IWDPs and E-Priority was set, more positive values of LRR_2 for five reservoirs and less negative values of LRR_1 are found in HJX, DJK, WFZ and XL reservoirs.
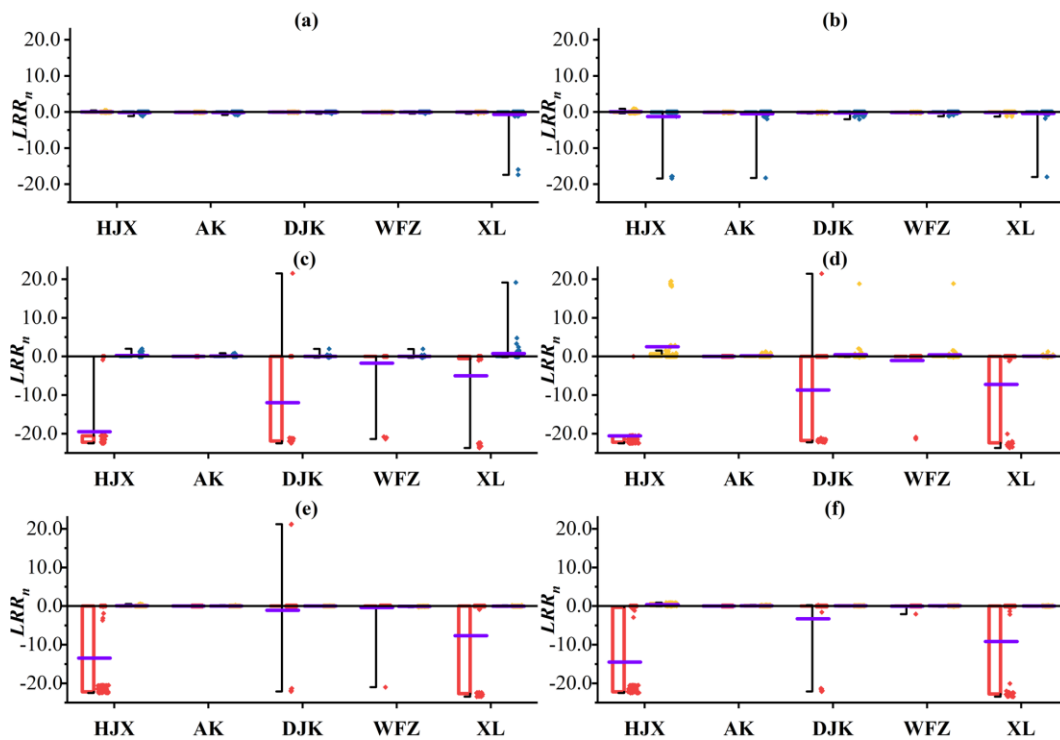

Figure 9. LRR_n with different highest priorities (i.e., between S_{m-1-n} and S_{m-4-n}) at the seasonal scale: (a) and (b) are LRR_n with the highest priority in S without IWDPs (i.e., between S_{0-1-n} and S_{0-4-n}) and with IWDPs (i.e., between S_{3-1-n} and S_{3-4-n}), (c) and (d) are LRR_n with the highest priority in H without IWDPs (i.e., between S_{0-2-n} and S_{0-4-n}) and with IWDPs (i.e., between S_{3-2-c} and S_{3-4-n}). (e) and (f) are LRR_n with the highest priority in E without IWDPs (i.e., between S_{0-3-n} and S_{0-4-n}) and with IWDPs (i.e., between S_{3-3-n} and S_{3-4-n}).

4.3.2 Responses of indexes in feedback loops with only water donation, water receiving, and both donation and receiving

To analyse the impacts of only water donation (i.e., S_{1-p-n} and S_{0-4-n}), only water receiving (i.e., S_{2-p-n} and S_{0-4-n}), and both donation and receiving (i.e., S_{3-p-n} and S_{0-4-n}) on feedback loops of SHE nexus across the multiple temporal and spatial scales, the differences of indexes between S_{m-p-n} and S_{0-4-n} are determined in a reservoirs group. The results of the monthly differences are shown in Figure 10-12. The seasonal results are shown in Figure 13. Corresponding annual-scale results can be found in Supplementary material Tables S3 -S5.

If there was only water donation and S-Priority was set, values of LRR_2 and LRR_3 for five reservoirs are negative and lower than those without IWDPs as shown in Figure 10 (a-1) and (a-2). More small negative values are found in DJK, water donation

strengthens the negative feedback of S on H and E for five reservoirs. If there was only water receiving and S-Priority was set, values of LRR_2 and LRR_3 for HJX and AK are the same as those without IWDPs. Meanwhile, for DJK, WFZ, and XL, the values are close to zero. XL exhibits a lot of positive values of LRR_3 as shown in Figure 10 (b-1) and (b-2). If there were both water donation and receiving, the mean values of LRR_2 for five reservoirs are all negative, and mean values of LRR_3 for five reservoirs are also negative, except XL as shown in Figure 10 (c-1) and (c-2). IWDPs strengthen the negative feedbacks of S on H and E for HJX, AK, DJK and WFZ and weakens the negative feedbacks of S on E for XL.
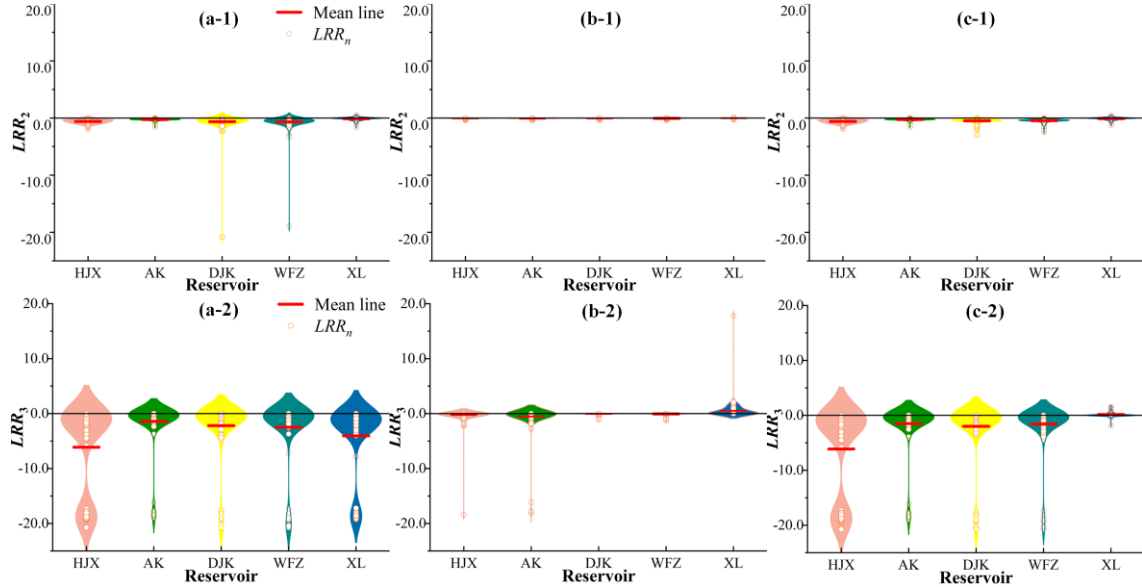
Figure 10. LRR_n values when there are different clusters of IWDPs and S-Priority was set at the monthly scale: (a-1) and (a-2) are LRR_2 and LRR_3 when there is only water donation (i.e., between S_{1-1-n} and S_{0-4-n}), (b-1) and (b-2) are LRR_2 and LRR_3 when there is only water receiving (i.e., between S_{2-1-n} and S_{0-4-n}), (c-1) and (c-2) are LRR_2 and LRR_3 when there are both donation and receiving (i.e., between S_{3-1-n} and S_{0-4-n}).

If there was only water donation and H-Priority was set, values of LRR_1 and LRR_3 for five reservoirs are lower than those without IWDPs as shown in Figure 11 (a-1) and (a-2). Negative values of LRR_3 for five reservoirs are found in low flow months such as November, December and January. Thus, water donation is found to strengthen the feedbacks of H on S and E, especially in low flow months. If there was only water receiving and H-Priority was set, values of LRR_1 and LRR_3 for DJK, WFZ and XL are greater than those without IWDPs as shown in Figure 11 (b-1) and (b-2). Water receiving weakens the feedbacks of H on S and E. If there were both water donation and receiving and H-Priority was set, the mean values of LRR_1 and LRR_3 for DJK, WFZ and XL are still lower than those without IWDPs. And the mean value of LRR_3 for XL is greater than those without IWDPs as shown in Figure 11 (c-1) and (c-2).
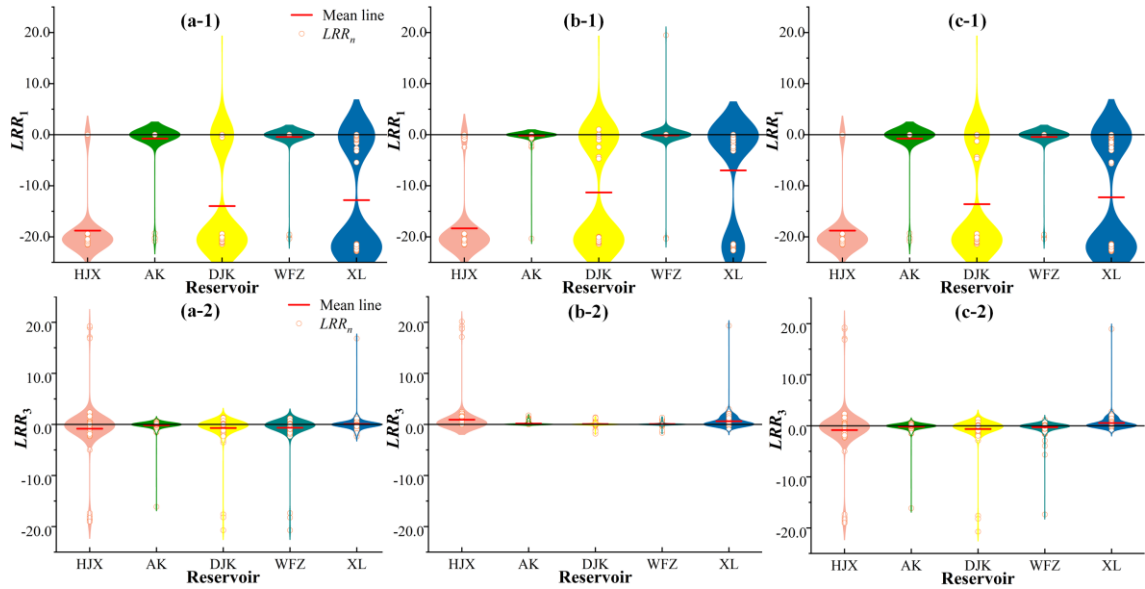
Figure 11. LRR_n values when there are different clusters of IWDPs and H-Priority was set at the monthly scale: (a-1) and (a-2) are LRR_2 and LRR_3 when there is only water donation (i.e., between S_{1-2-n} and S_{0-4-n}), (b-1) and (b-2) are LRR_2 and LRR_3 when there is only water receiving (i.e., between S_{2-2-n} and S_{0-4-n}), (c-1) and (c-2) are LRR_2 and LRR_3 when there are both donation and receiving(i.e., between S_{3-2-n} and S_{0-4-n}).

If there was only water donation and E-Priority was set, then values of LRR_1 and LRR_2 for five reservoirs are shown in Figure 12 (a-1) and (a-2). The mean values of LRR_1 and LRR_2 for these five reservoirs are all negative, and all these values are lower than the those without IWDPs. Different from the values of LRR_n without IWDPs, there are no positive values of LRR_1 for DJK and few positive values of LRR_2 for five reservoirs due to the decreased inflows from upstream with water donation. If there was only water receiving and E-Priority was set, values of LRR_1 and LRR_2 for DJK, WFZ and XL are greater than those without IWDPs. If there were both water donation and receiving and E-Priority was set, the mean values of LRR_1 and LRR_2 for DJK, WFZ and XL are still lower than those without IWDPs as shown in Figure 12 (c-1) and (c-2).
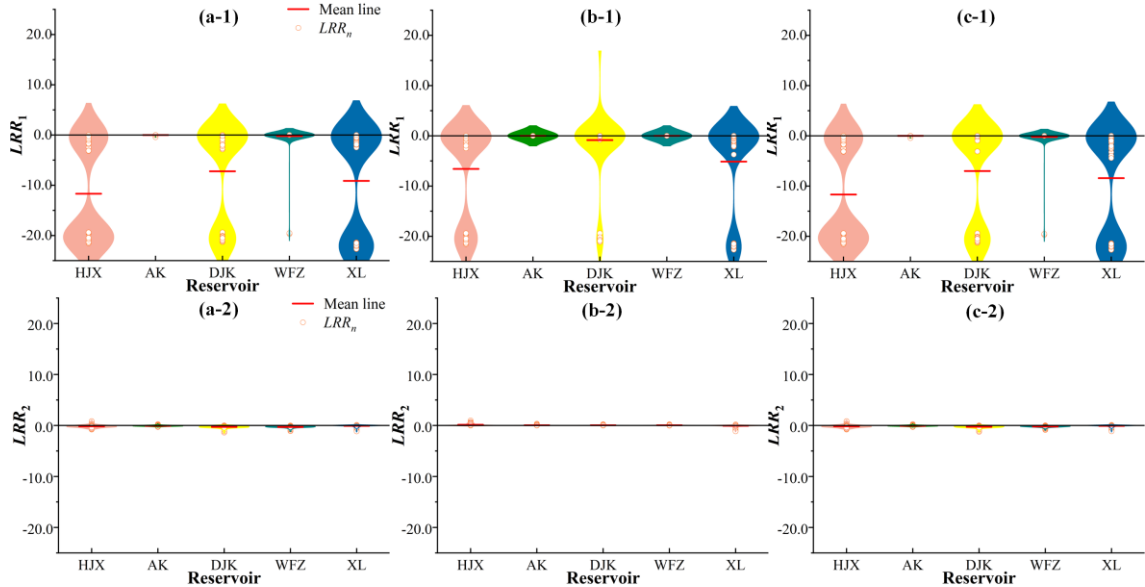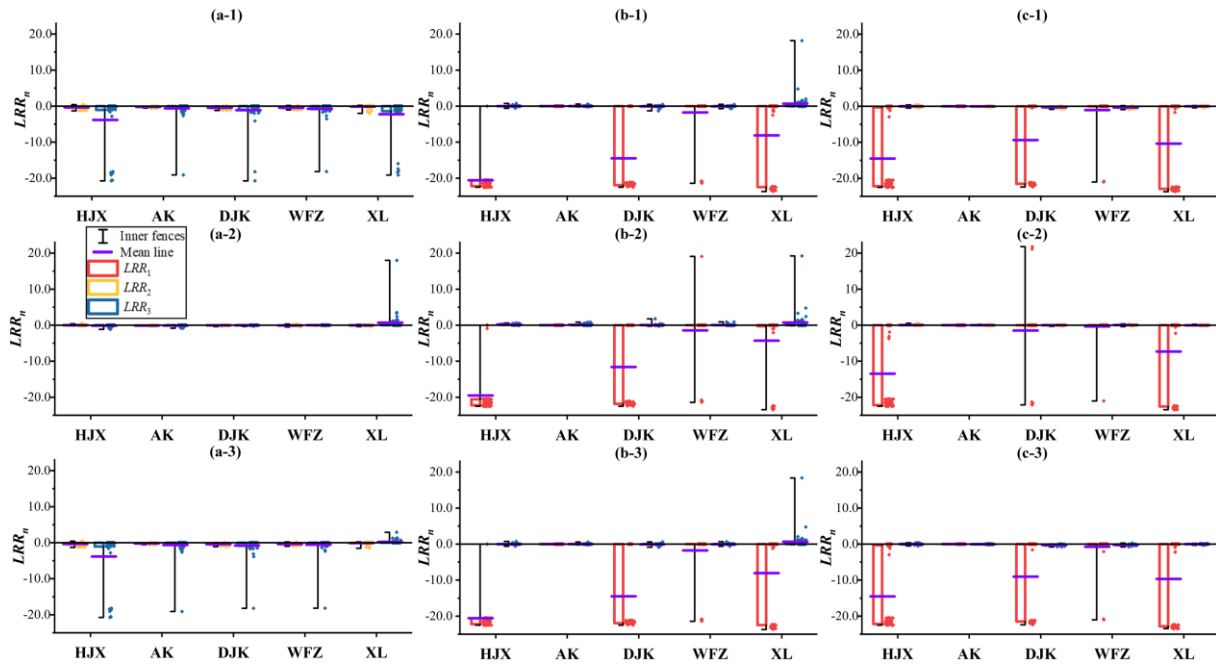

Figure 12. LRR_n values when there are different clusters of IWDPs and E-Priority was set at the monthly scale: (a-1) and (a-2) are LRR_1 and LRR_2 when there is only water donation (i.e., between S_{1-3-n} and S_{0-4-n}), (b-1) and (b-2) are LRR_1 and LRR_2 when there is only water receiving (i.e., between S_{2-3-n} and S_{0-4-n}), (c-1) and (c-2) are LRR_1 and LRR_2 when there are both donation and receiving (i.e., between S_{3-3-n} and S_{0-4-n}).

If there was only water donation and S-Priority was set, values of LRR_2 and LRR_3 as shown in Figure 13(a-1) are lower than those without IWDPs in all seasons as shown in Figure 9 (a). If there was only water receiving and S-Priority was set,

20

mean values of LRR_2 and LRR_3 for DJK, WFZ and XL as shown in Figure 13 (a-2) are all greater than those without IWDPs. If there were both water donation and receiving and S-Priority was set, mean values of LRR_2 for five reservoirs decrease compared to those without IWDPs. Mean values of LRR_3 for HJX, AK, DJK and WFZ decrease but for XL it increases compared to those without IWDPs as shown in Figure 13 (a-3). If there was only water donation and H-Priority was set, values of LRR_1 and LRR_3 as shown in Figure 13(b-1) are lower than those without IWDPs. Water donation strengthens feedbacks of H on S for HJX, DJK and XL. If there was only water receiving and H-Priority was set, mean values of LRR_2 for DJK, WFZ and XL increase, while mean values of LRR_3 for DJK, WFZ and XL only increase slightly compared to those without IWDPs. If there were both water donation and receiving and H-Priority was set, mean values of LRR_2 for five reservoirs are negative or zero (AK), and mean values of LRR_3 for five reservoirs are close to zero except XL as shown in Figure 13 (b-3). If there was only water donation and E-Priority was set, it can be found that values of LRR_1 and LRR_2 in all seasons are lower than those without IWDPs as shown in Figure 13(c-1). Mean values of LRR_1 and LRR_2 for five reservoirs all decrease. If there was only water receiving and E-Priority was set, mean values of LRR_1 and LRR_2 for DJK, WFZ and mean values of LRR_1 for XL are greater than those without IWDPs, while mean values of LRR_2 for XL get an increase as shown in Figure 13 (c-2). If there were both water donation and receiving and E-Priority was set, Values of LRR_1 and LRR_2 for DJK and WFZ and values of LRR_1 for XL as shown in Figure 13 (c-3) are greater than those with only water donation, while lower than those without IWDPs. While values of LRR_2 for XL are greater than those without IWDPs because of the reduced spilled water. Therefore, values of LRR_n at seasonal scale demonstrate a consistent conclusion with those at the monthly scale. Moreover, the values of LRR_n are relatively stable in summer, while they change greatly in winter at seasonal scale. The impacts of IWDPs on SHE nexus are more significant in low flow seasons.


Figure 13. LRR_n values when there are different clusters of IWDPs at the seasonal scale: (a-1), (a-2) and (a-3) are LRR_n when there was only water donation, when there was only water receiving, when there were both donation and receiving and S-Priority was set (i.e., between S_{m-1-n} and S_{0-4-n}); (b-1), (b-2) and (b-3) are those when H-Priority was set (i.e., between S_{m-2-n} and S_{0-4-n}); (c-1), (c-2) and (c-3) are those when E-Priority was set (i.e., between S_{m-3-n} and S_{0-4-n}).

4.4 Responses of the three components with IWDPs

To identify the impacts of IWDPs on S, H and E components in a reservoirs group, differences between indexes without IWDPs and with IWDPs (i.e., S_{3-4-n} and S_{0-4-n}) are determined. Negative values of LRR_1 for five reservoirs are found in all months as shown in Figure 14 (a). It is found that values of LRR_1 for DJK are significantly smaller than those for other reservoirs.

Mean values of LRR_2 for five reservoirs are all negative as shown in Figure 14 (b). Positive values of LRR_3 are found in XL and negative values of LRR_3 are found in HJX, AK, DJK and WFZ in all months, as shown in Figure 14 (c).
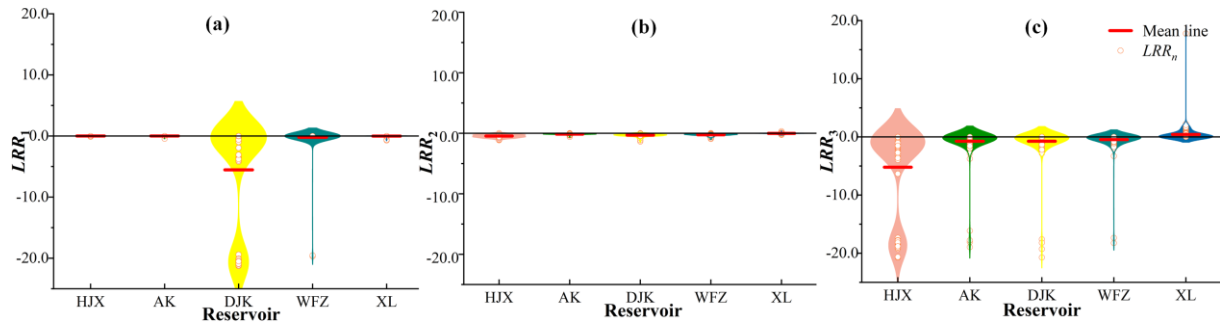
Figure 14. the differences of indexes (i.e., (a) LRR_1, (b) LRR_2, (c) LRR_3 for log response ratio of the S, H, and E component) between S_{3-4-n} and S_{0-4-n} at the monthly scale.

5 Discussion

The proposed framework reveals significant negative feedbacks of the water supply (S) on both hydropower generation (H) and environment conservation (E), as evidenced by reductions in hydropower generation (negative LRR_2 in Figure 7 (a-1)) and ecological flow satisfaction rate (negative LRR_2 in Figure 7 (a-2)) with S-Priority. The negative feedbacks of the S component on E are more pronounced than those on H, as evidenced by the wider range of variation in LRR_3 values compared to LRR_2 values. These findings are consistent with previous studies on the SHE nexus (Chen et al.,2018; Khalkhali et al., 2018). It has been found that there are a few positive feedbacks between S and H in abundant water months because the increased spilled water leads to a reduction in hydropower generation (Jiang et al., 2018). Thus, the increasing water storage or increasing water supply still can ensure hydropower generation. The values of ecological flow satisfaction rates for XL and AK significantly decrease due to their greater reductions of ecological flow and their higher ecological flow standards at the two reservoir dam sites. The extreme values (e.g., lower than 90 % months values) of LRR_3 for HJX, AK, WFZ, and XL reservoirs occur in the higher water supply demand months such as June to September of each year. And Gao et al. (2023) find that the higher water supply demand, the lower ecological flow left in river. The environment conservation of downstream river systems is critically influenced by upstream water supply decisions (Gupta, 2008). Contrary to the unidirectional positive nexus between hydropower generation and environment conservation proposed by Wei et al. (2022), our study reveals bidirectional feedbacks of H and E, aligning with Wu et al. (2021). The positive feedbacks between H and E are weakened or even turn to be negative in the small installed hydropower generation capacity reservoirs (e.g., the XL reservoir, Zhang et al., 2008) even in abundant water months, particularly. The increased flows for hydropower generation alleviate the pressure of ecological damage in river. However, the more flows for hydropower generation from the reservoir, the less available water resources for supply (Doummar et al., 2009), and leads to negative impacts on the S component. The feedbacks of the H on S are more pronounced than on E, according to the wider range of variation in LRR_1 values compared to LRR_3 values. Negative feedbacks of the E component on S for reservoirs has been found when the main function is water supply while no significant effect on reservoirs has been found when the main function is hydropower generation (negative LRR_1 in Figure 7 (c-1)). There are both negative and positive feedbacks of the E component on H while the negative feedbacks strengthen in abundant water months. Feedbacks of the E component on S are stronger than those on H, according to the values of LRR_n. The negative feedbacks between S and H, and between S and E are strong in low flow months due to the high-water supply demand. Stronger competition for water among S, H and E occurs in low flow months, with stronger negative feedbacks of the SHE nexus (Wu et al., 2021). Feedback loops of SHE nexus in reservoirs with regulation function (e.g., AK and DJK) remain stable under the varying inflow conditions.

These reservoirs reasonably allocate water among S, H and E components to prevent strengthening of negative feedbacks in low flow months. Furthermore, increasing hydropower generation flow might have impacts on downstream water quality and biodiversity (Botelho et al., 2017; Martinez et al., 2019), the feedbacks of H on E are enhanced.

550　　　Inter-basin water diversion projects (IWDPs) have negative impacts on the regional water supply from DJK and upstream reservoirs with negative LRR_1, consistent with Hong et al. (2016) and Ouyang et al. (2018). All reservoirs experience reduced hydropower generation, but there are positive impacts on H in abundant water months (positive LRR_2 in Figure 14 (b)). Many studies have highlighted the negative impacts of IWDPs on hydropower generation (Yang, et al., 2023), but the positive impacts are less frequently discussed. With the water donation for the Han-to-Wei Water Diversion Project, the Middle Route of the

555　　South-to-North Water Diversion Project and the Northern Hubei Water Resources Allocation Project, multiple algal bloom events occurred downstream of HRB (Tian et al., 2022), the water donation having a significant negative impact on the environment conservation of the basin. Water received from the Three Gorges Reservoir to Hanjiang River are not compensate for all their negative impacts, and water receiving from the Changjiang-to-Hanjiang River Water Diversion Project benefits environment conservation for XL. It is evident that IWDPs significantly alter the feedback loops of the SHE nexus by modifying

560　　water availability. As IWDPs export or import water to or from an area, the amount of available water changes, and can prompt a redistribution and re-planning of the available water (Li, et al., 2014), which can significantly impact on feedback loops of SHE nexus (Feng, et al., 2019). Although strong responses occur in feedback loops of the SHE nexus, its positive or negative nature of feedback among these components remains stable with impacts of IWDPs. Thus, the redistribution and re-planning of available water can not alter their competition or synergy among the components of the SHE nexus. It is evident that water

565　　donation strengthens the negative feedbacks between S and H, the negative feedbacks between S and E, and the positive feedbacks between H and E, while receiving water weakens these feedbacks. Water donation results in a reduction of available water (Mok et al., 2015; Wu et al., 2022), leads to lower flow, stronger competition for water among S, H and E, and strengthens the feedbacks. Reduced competition among S, H and E is found in water receiving areas, primarily due to the replenishing available water resources. The persistent feedback polarity with IWDPs suggests that simply increasing water receiving (e.g.,

570　　via compensation donations like the Three Gorges Reservoir to Hanjiang River) cannot resolve inherent SHE conflicts—instead, adaptive allocation rules that account for these stable feedback patterns are needed.

　　　　The consistency in the signs of mean LRR_n values across seasonal as shown in Figures 9 and 13 and annual scales as shown in Supplementary material Table S1-S5 with those at the monthly scale indicates an inherent similarity and stability in SHE nexus feedback loops over different temporal resolutions. Compared with the values of LRR_n at monthly scale, the values at the

575　　seasonal scale show stronger periodic variations. Based on the variations in LRR_n and the mathematical implications of LRR_1, LRR_2, and LRR_3, this study found that these periodic variations align closely with the runoff variations, and the temporal and spatial variations in feedback loops are primarily attributed to variations in runoff. The wavelet transform analysis has also been applied in the runoff for HJX, AK, DJK, WFZ, and XL dam sites. The results are consistent with those of the Hutuo River Basin (Xu et al., 2018), the periodic variations being at the seasonal scale. The LRR_n values at the seasonal scale can help analyze the

580　　variations in periodic feedback loops. Different from the monthly or seasonal scales, results at the annual scale reveal the long-term trends and periodic variations in the inter-annual and spatial trends of the SHE nexus from a macro perspective. The impacts of reservoir operation and the regulation on SHE nexus can be clearly simulated and observed at the monthly scale, so the immediate changes in the nexus at monthly scale can provide information for short-term decision-making in reservoirs.

6 Conclusions

585　　A framework is proposed to address the different impacts of IWDPs on the dynamic SHE nexus across the multiple temporal

and spatial scales in reservoirs group with different priority functions and to explore synergies in feedback loops. The HRB was taken as a case study to verify the feasibility and reliability of this framework. Negative feedbacks can be found between S and H, and between S and E while positive feedbacks can be found between H and E in a reservoirs group without IWDPs. The negative feedbacks of S on H and the positive feedbacks of E on H are weakened or even broken in abundant water periods. All feedback loops are strengthened in low flow periods due to heightened competition for water resources. Water donation strengthens the negative feedbacks between S and H, the negative feedbacks between S and E, and the positive feedbacks between H and E, while water receiving weakens these feedbacks. Feedback loops of the SHE nexus exhibit intrinsic similarity and stability across different time scales. The impact of reservoir operation and regulation on the SHE nexus are clearest at the monthly scale. The seasonal scale reveals variations in periodic feedback loops. And the annual scale offers inter-annual and spatial trends of the SHE nexus from a macro perspective. Feedback loops in reservoirs with regulation function (e.g., AK and DJK) remain stable under the varying inflow conditions at monthly scale. The positive feedbacks between H and E are weakened or even turn to be negative in the small installed hydropower generation capacity reservoirs (e.g., the XL reservoir) even in abundant water periods. Feedback loops for downstream reservoirs are influenced by their upstream reservoirs, especially in low flow periods. In abundant water periods, the increasing water donation or regional water supply can increase hydropower generation efficiency due to the reduced spilled water. In dry periods, it is necessary to consider the priority order of S, H, and E, and determine water utilization threshold for each component to maximize the benefits. We find that simply increasing water receiving cannot resolve inherent SHE conflicts because of the persistent feedback polarity with IWDPs. Adaptive allocation rules are needed that account for these stable feedback patterns.

This framework offers a systematic and quantitative approach to examining the spatiotemporal variations of SHE nexus with external perturbations. It elucidates the existence and nature of synergies among S, H, and E. However, more work should be done to enrich the representation of every component such as the E component. This component should be enriched by a comprehensive set of water quality indicators. Then more details of the mechanism of the SHE nexus can be elaborated.

References

Bai, T., Li, L., Mu, P., Pan, B., and Liu, J.: Impact of Climate Change on Water Transfer Scale of Inter-basin Water Diversion

Project, Water Resour. Manag., 37(6-7), 2505-2525, https://doi.org/10.1007/s11269-022-03387-8, 2023.

Bland, M.J.A.G.: Statistical methods for assessing agreement between two methods of clinical measurement, Lancet 1(8476),
625   307-310, https://doi.org/10.1016/S0140-6736(86)90837-8, 1986.

Botelho, A., Ferreira, P., Lima, F., Pinto, L.M.C., and Sousa, S.: Assessment of the environmental impacts associated with hyd
ropower. Renew. Sust. Energ. Rev. 70, 896-904. https://doi.org/10.1016/j.rser.2016.11.271, 2017.

Gao, Y., Xiong, W., and Wang, C.: numerical modelling of a dam-regulated river network for balancing water supply and ecol
ogical flow downstream, Water, 15(10):1962, https://doi.org/10.3390/W15101962, 2023.

630   Chen, Y., Mei, Y., Cai, H., and Xu, X.: Multi-objective optimal operation of key reservoirs in Ganjiang River oriented to powe
r generation, water supply and ecology, J. Hydraul. Eng., 49(05):628-638, https://doi.org/10.13243/j.cnki.slxb.20180130, 2
018. (in Chinese)

Chung, M., Frank, K.A., Pokhrel, Y., Dietz, T., and Liu, J.: Natural infrastructure in sustaining global urban freshwater ecosys
tem services, Nat. Sustain., 4(12), 1068-1075, https://doi.org/10.1038/s41893-021-00786-4, 2021.

635   Conway, D., van Garderen, E. A., Deryng, D., Dorling, S., Krueger, T., Landman, W., Lankford, B., Lebek, K., Osborn, T., Ri
ngler, C., Thurlow, J., Zhu, T., and Dalin, C.: Climate and southern Africa's water-energy-food nexus, Nat. Clim. Chang., 5
(9), 837-846, https://doi.org/10.1038/NCLIMATE2735, 2015.

Gupta, D. A.: Implication of environmental flows in river basin management. Physics and Chemistry of the Earth, Phys. Che
m. Earth., 33(5):298-303, https://doi.org/10.1016/j.pce.2008.02.004, 2008.

640   Dong, J., Chen, X., Li, Y., Gao, M., Wei, L., Tangdamrongsu, N., Crow, T.W.: Inter-Basin Water Transfer Effectively Compen
sates for Regional Unsustainable Water Use. Water Resour. Res., 59(12), https://doi.org/10.1029/2023WR035129, 2023.

Dong, Q., Zhang, X., Chen, Y., and Fang, D.: Dynamic Management of a Water Resources-Socioeconomic-Environmental Sy
stem Based on Feedbacks Using System Dynamics, Water Resour. Manag., 33(6), 2093-2108, https://doi.org/10.1007/s112
69-019-02233-8, 2019.

645   Doummar, J., Massoud, M.A., Khoury, R., and Khawlie, M.: Optimal Water Resources Management: Case of Lower Litani Ri
ver, Lebanon, Water Resour. Manag., 23(11), 2343-2360, https://doi.org/10.1007/s11269-008-9384-z, 2009.

Endo, A., Tsurita, I., Burnett, K., and Orencio, P.M.: A review of the current state of research on the water, energy, and food ne
xus, J. Hydrol. Reg. Stud., 11, 20-30, https://doi.org/10.1016/j.ejrh.2015.11.010, 2017.

FAO.: The water-energy-food nexus-A new approach in support of food security and sustainable agriculture, Rome: Food and
650   Agriculture Organization of the United Nations, 2014.

Feng, M., Liu, P., Guo, S., Yu, J.D., Cheng, L., Yang, G., and Xie, A.: Adapting reservoir operations to the nexus across water
supply, power generation, and environment systems: An explanatory tool for policy makers, J. Hydrol., 574, 257-275,
https://doi.org/10.1016/j.jhydrol.2019.04.048, 2019.

Franchini, M., Ventaglio, E., and Bonoli, A.: A Procedure for Evaluating the Compatibility of Surface Water Resources with E
655   nvironmental and Human Requirements, Water Resour. Manag., 25(14), 3613-3634, https://link.springer.com/article/10.10
07/s11269-011-9873-3, 2011.

Gou, J., Miao, C., Duan, Q., Tang, Q., Di, Z., Liao, W., Wu, J., and Zhou, R.: Sensitivity Analysis-Based Automatic Parameter
Calibration of the VIC Model for Streamflow Simulations Over China, Water Resour. Res., 56(1), https://doi.org/10.1029
/2019WR025968, 2020.

660   He, Y.Y., X, F.: Study of water resources allocation model of North Hubei Water Transfer Project and operation schemes comp
arison, Express Water Resources & Hydropower Information, 41(10), 26-29, https://doi.org/10.15974/j.cnki.slsdkb.2020.1
0.005, 2020.

Hong, X., Guo, S., Le Wang, Yang, G., Liu, D., Guo, H., and Wang, J.: Evaluating Water Supply Risk in the Middle and Lowe

r Reaches of Hanjiang River Basin Based on an Integrated Optimal Water Resources Allocation Model, Water, 8(9), 364, https://doi.org/10.3390/w8090364, 2016.

Jiang, Z., Wu, W., Qin, H., and Zhou, J.: Credibility theory based panoramic fuzzy risk analysis of hydropower station operation near the boundary, J. Hydrol., 565, 474-488, https://doi.org/10.1016/j.jhydrol.2018.08.048, 2018.

Kattel, G.R., Shang, W., Wang, Z., and Langford, J.: China's South-to-North Water Diversion Project Empowers Sustainable Water Resources System in the North, Sustainability, 11(13), 3735, https://doi.org/10.3390/su11133735, 2019.

Keyhanpour, M. J., Jahromi, S. H. M., and Ebrahimi, H.: System dynamics model of sustainable water resources management using the Nexus Water-Food-Energy approach, Ain Shams Eng. J., 12(2), 1267-1281, https://doi.org/10.1109/MCDM.2007.369107, 2021.

Khalkhali, M., Westphal, K., and Mo, W.: The water-energy nexus at water supply and its implications on the integrated water and energy management, Sci. Total Environ., 636, 1257-1267, https://doi.org/10.1016/j.scitotenv.2018.04.408, 2018.

Koohi, S., Azizian, A., and Brocca, L.: Calibration of a Distributed Hydrological Model (VIC-3L) Based on Global Water Resources Reanalysis Datasets, Water Resour. Manag., 36(4), 1287-1306, https://doi.org/10.1007/s11269-022-03081-9, 2022.

Li, C., and Kang, L.: A New Modified Tennant Method with Spatial-Temporal Variability, Water Resour. Manag., 28(14), 4911-4926, https://doi.org/10.1007/s11269-014-0746-4, 2014.

Li, C., Kang, L., Zhang S., Zhou, L.: A Modified FDC Method with Multi-level Ecological Flow Criteria, J. Yangtze River Sci. Res. Inst., 32 (11): 1-6, 13, https://doi.org/10.11988 /ckyyb.20140814, 2015. (in Chinese)

Li, Y., Xiong, W., Zhang, W., Wang, C., and Wang, P.: Life cycle assessment of water supply alternatives in water -receiving areas of the South-to-North Water Diversion Project in China, Water Res., 89, 9-19, https://doi.org/10.1007/s11269-011-9873-3, 2016.

Liang, X., and Lettenmaier, D.P.: Wood, E.F., Burges, S.J.: A Simple Hydrologically Based Model Of Land-Surface Water And Energy Fluxes For General-Circulation Models, J. Geophys. Res.-Atmos., 99(D7), 14415-14428, https://doi.org/10.1029/94JD00483, 1994.

Liu, D., Guo, S., Shao, Q., Liu, P., Xiong, L., Wang, L., Hong, X., Xu, Y., and Wang, Z.: Assessing the effects of adaptation measures on optimal water resources allocation under varied water availability conditions, J. Hydrol., 556, 759-774, https://doi.org/10.1016/j.jhydrol.2017.12.002, 2018.

Liu, J., Yuan, X., Zeng, J., Jiao, Y., Li, Y., Zhong, L., and Yao, L.: Ensemble streamflow forecasting over a cascade reservoir catchment with integrated hydrometeorological modeling and machine learning, Hydrol. Earth Syst. Sci., 26, 265–278, https://doi.org/10.5194/hess-26-265-2022, 2022.

Long, D., Yang, W., Scanlon, B.R., Zhao, J., Liu, D., Burek, P., Pan, Y., You, L., and Wada, Y.: South-to-North Water Diversion stabilizing Beijing's groundwater levels, Nat. Commun. 11(1), 3665, https://doi.org/10.1038/s41467-020-17428-6, 2020.

MacGREGOR, J.J.: Natural Resources in the United States, Nature, 200(4906), 518-520, https://doi.org/10.1038/200518a0, 1963.

Mansour, F., Al-Hindi, M., Najm, M.A., and Yassine, A.: The water energy food nexus: A multi-objective optimization tool, Comput. Chem. Eng., 187, 108718, https://doi.org/10.1016/J.COMPCHEMENG.2024.108718, 2024.

Martinez, J., Deng, Z., Tian, C., Mueller, R., Phonekhampheng, O., Singhanouvong, D., Thorncraft, G., Phommavong, T., and Phommachan, K.: In situ characterization of turbine hydraulic environment to support development of fish-friendly hydropower guidelines in the lower Mekong River region, Ecol. Eng., 133, 88-97, https://doi.org/10.1016/j.ecoleng.2019.04.028, 2019.

Mok, K.Y., Shen, G., and Yang, J.: Stakeholder management studies in mega construction projects: A review and future directions, Int. J. Proj. Manag., 33(2), 446-457, https://doi.org/10.1016/j.ijproman.2014.08.007, 2015.

705 Mu, L., Bai, T., Liu, D., and Li, L.: Impact of Climate Change on Water Diversion Risk of Inter-Basin Water Diversion Project, Water Resour. Manag., 38(8), 2731-2752, https://doi.org/10.1007/s11269-024-03777-0, 2024.

Nash, J.E.S.J., River flow forecasting through conceptual models part I — A discussion of principles, J. Hydrol., 3(10), 282-290, https://doi.org/10.1016/0022-1694(70)90255-6, 1970.

Ouyang, S., Qin, H., Shao, J., Zhang, R., and Dai, M.: Operation Mode of Danjiangkou Reservoir under Water Diversion Conditions of South-to-North Water Diversion Middle Route Project, IOP Conf. Ser.: Mater. Sci. Eng., 366(1), https://doi.org/10.1088/1757-899X/366/1/012010, 2018.

Ouyang, S., Qin, H., Shao, J., Lu, J., Bing, J., Wang, X., and Zhang, R.: Multi-objective optimal water supply scheduling model for an inter-basin water transfer system: the South-to-North Water Diversion Middle Route Project, China, Water Supply, 20(2), 550-564, https://doi.org/10.2166/ws.2019.187, 2020.

715 Patrick, C.J., Kominoski, J.S., McDowell, W.H., Branoff, B., Lagomasino, D., Leon, M., Hensel, E., Hensel, M.J.S., Strickland, B.A., Aide, T.M., Armitage, A., Campos-Cerqueira, M., Congdon, V.M., Crowl, T.A., Devlin, D.J., Douglas, S., Erisman, B.E., Feagin, R.A., Geist, S.J., Hall, N.S., Hardison, A.K., Heithaus, M.R., Hogan, J.A., Hogan, J.D., Kinard, S., Kiszka, J.J., Lin, T., Lu, K., Madden, C.J., Montagna, P.A., O'Connell, C.S., Proffitt, C.E., Reese, B.K., Reustle, J.W., Robinson, K.L., Rush, S.A., Santos, R.O., Schnetzer, A., Smee, D.L., Smith, R.S., Starr, G., Stauffer, B.A., Walker, L.M., Weaver, C.A., Wetz, M.S., Whitman, E.R., Wilson, S.S., Xue, J., and Zou, X.: A general pattern of trade-offs between ecosystem resistance and resilience to tropical cyclones, Sci. Adv., 8(9), eabl9155, https://doi.org/10.1126/sciadv.abl9155, 2022.

Qiu, H., Chen, L., Zhou, J., He, Z., and Zhang, H.: Risk analysis of water supply-hydropower generation-environment nexus in the cascade reservoir operation, J. Clean. Prod., 283, 124239, https://doi.org/10.1016/j.jclepro.2020.124239, 2021.

Quer, A.M.I., Larsson, Y., Johansen, A., Arias, C.A., and Carvalho, P.N.: Cyanobacterial blooms in surface waters - Nature-based solutions, cyanotoxins and their biotransformation products, Water Res., 251, 121122, https://doi.org/10.1016/j.watres.2024.121122, 2024.

Rousseeuw, P.J.A.L.: Robust Regression and Outlier Detection, John Wiley & Sons, New York, https://doi.org/10.1002/0471725382, 1987.

Sanders, K.T., and Webber, M.E.: Evaluating the energy consumed for water use in the United States, Environ. Res. Lett., 7(3), 034034, https://doi.org/10.1088/1748-9326/7/3/034034, 2012.

Sheng, J., Zhang, R., and Yang, H.: Inter-basin water transfers and water rebound effects: The South-North water transfer Project in China. J. Hydrol., 638, 131516, https://doi.org/10.1016/J.JHYDROL.2024.131516, 2024.

Siddik, M.A.B., Dickson, K.E., Rising, J., Ruddell, B.L., and Marston, L.T.: Interbasin water transfers in the United States and Canada, Sci. Data, 10(1), 27, https://doi.org/10.1038/s41597-023-01935-4, 2023.

735 Stickler, C.M., Coe, M.T., Costa, M.H., Nepstad, D.C., McGrath, D.G., Dias, L.C.P., Rodrigues, H.O., and Soares-Filho, B.S.: Dependence of hydropower energy generation on forests in the Amazon Basin at local and regional scales, Proceedings of the National Academy of Sciences, 110(23), 9601-9606, https://doi.org/10.1073/pnas.1215331110, 2013.

Stone, R., and Jia, H.: Hydroengineering - Going against the flow. Science, 313(5790), 1034-1037, https://doi.org/10.1126/science.313.5790.1034, 2006.

740 Su, L., Lettenmaier, P.D., Pan, M., and Bass, B. Improving runoff simulation in the Western United States with Noah-MP and VIC models, Hydrol. Earth Syst. Sci., 28, 3079–3097, https://doi.org/10.5194/hess-28-3079-2024, 2024.

Tang, M., Xu, W., Zhang, C., Shao, D., Zhou, H., and Li, Y.: Risk assessment of sectional water quality based on deterioration rate of water quality indicators: A case study of the main canal of the Middle Route of South-to-North Water Diversion Project, Ecol. Indic., 135, 108776, https://doi.org/10.1016/j.ecolind.2022.108592, 2022.

745 Tang, X., Huang, Y., Pan, X., Liu, T., Ling, Y., and Peng, J.: Managing the water-agriculture-environment-energy nexus: Trade

-offs and synergies in an arid area of Northwest China, Agric. Water Manag. 295, 108776, https://doi.org/10.1016/j.agwat.2024.108776, 2024.

Tao, H., Gemmer, M., Song, Y., and Jiang, T.: Ecohydrological responses on water diversion in the lower reaches of the Tarim River, China., Water Resour. Res., 44(8), https://doi.org/10.1029/2007WR006186, 2008.

Tauro, F.: River basins on the edge of change Water scarcity after the Millennium Drought reveals the finite resilience of water systems, Science, 372(6543), 680-681, https://doi.org/10.1126/science.abi8770, 2021.

Tennant, D.L.: Instream Flow Regimens for Fish, Wildlife, Recreation and Related Environmental Resources, Fisheries, 4(1), 6-10, https://doi.org/10.1577/1548-8446(1976)001<0006:IFRFFW>2.0.CO;2, 1976.

Tharme, R.E.: A global perspective on environmental flow assessment: Emerging trends in the development and application of environmental flow methodologies for rivers. River Res. Appl, 19(5-6), 397-441, https://doi.org/10.1002/rra.736, 2003.

Tian, J., Guo, S.L., Wang, J., Wang, H.Y., Pan, Z.K.: Preemptive warning and control strategies for algal blooms in the downstream of Han River, China, Ecol. Indic., 142: 109190, https://doi.org/10.1016/J.ECOLIND.2022.109190, 2022.

Wang, C., Li, Z., Ni, X., Shi, W., Zhang, J., Bian, J., and Liu, Y.: Residential water and energy consumption prediction at hourly resolution based on a hybrid machine learning approach, Water Res., 246, 120733, https://doi.org/10.1016/j.watres.2023.120733, 2023.

Wang, G., Zhang, J., Jin, J., Pagano, T.C., Calow, R., Bao, Z., Liu, C., Liu, Y., Yan, X.: Assessing water resources in China using PRECIS projections and a VIC model. Hydrol. Earth Syst. Sci., 16(150):231-240, https://doi.org/10.5194/hess-16-231-2012, 2012.

Wang, H., Liu, J., Klaar, M., Chen, A., Gudmundsson, L., and Holden, J.: Anthropogenic climate change has influenced global river flow seasonality, Science, 383(6686), 1009-1014, https://doi.org/10.1126/science.adi9501, 2024.

Wei, J., Zhang, Q., Yin, Y., Peng, K., Wang, L., Cai, Y., and Gong, Z.: Limited Impacts of Water Diversion on Micro-eukaryotic Community along the Eastern Route of China's South-to-North Water Diversion Project, Water Res., 262, 122109, https://doi.org/10.1016/j.watres.2024.122109, 2024.

Wei, N., Yang, F.L., Lu, K.M., Xie, J.C., Zhang, S.F.: A Method of Multi-Objective Optimization and Multi-Attribute Decision-Making for Huangjinxia Reservoir, Appl. Sci., 12(13):6300, https://doi.org/10.3390/APP12136300, 2022.

Wei, X., Zhang, H., Singh, V.P., Dang, C., Shao, S., and Wu, Y.: Coincidence probability of streamflow in water resources area, water receiving area and impacted area: implications for water supply risk and potential impact of water transfer, Hydrol. Res., 51(5), 1120-1135, https://doi.org/10.2166/nh.2020.106, 2020.

Wu, J., Luo, J., Du, X., Zhang, H., and Qin, S.: Optimizing water allocation in an inter-basin water diversion project with equity-efficiency tradeoff: A bi-level multiobjective programming model under uncertainty, J. Clean. Prod., 371, 133606, https://doi.org/10.1016/j.jclepro.2022.133606, 2022.

Wu, Z., Liu, D., Mei, Y., Guo, S., Xiong, L., Liu, P., Chen, J., Yin, J., and Zeng, Y.: A nonlinear model for evaluating dynamic resilience of water supply hydropower generation-environment conservation nexus system. Water Resour. Res., 59, e2023WR034922. https://doi.org/10.1029/2023WR034922, 2023.

Wu, Z., Mei, Y., Cheng, B., and Hu, T.: Use of a Multi-Objective Correlation Index to Analyze the Power Generation, Water Supply and Ecological Flow Mutual Feedback Relationship of a Reservoir, Water Resour. Manag., 35(2), 465-480. https://doi.org/10.1007/s11269-020-02726-x, 2021.

Xia, R., Wang, G., Zhang, Y., Yang, P., Yang, Z., Ding, S., Jia, X., Yang, C., Liu, C., Ma, S., Lin, J., Wang, X., Hou, X., Zhang, K., Gao, X., Duan, P., and Qian, C.: River algal blooms are well predicted by antecedent environmental conditions, Water Res., 185, 116221, https://doi.org/10.1016/j.watres.2020.116221, 2020.

Xu, F., Jia, Y., Niu, C., Liu, J., and Hao, C.: Changes in Annual, Seasonal and Monthly Climate and Its Impacts on Runoff in t

he Hutuo River Basin, China, Water, 10(3), w10030278, https://doi.org/10.3390/w10030278, 2018.

Yan, Z., Zhou, Z., Liu, J., Wen, T., Sang, X., and Zhang, F.: Multiobjective Optimal Operation of Reservoirs Based on Water Supply, Power Generation, and River Ecosystem with a New Water Resource Allocation Model, J. Water Resour. Plan. Manage. -Asce,146(12), https://doi.org/10.1061/(ASCE)WR.1943-5452.0001302, 2020.

Yeste, P., Ojeda, G.M., Gámiz-Fortis, R.S., Castro-Díez, Y., Bronstert, A., and Esteban-Parra, J.M.: A large-sample modelling approach towards integrating streamflow and evaporation data for the Spanish catchments, Hydrol. Earth Syst. Sci., 28, 5331–5352, https://doi.org/10.5194/hess-28-5331-2024, 2024.

Yang, Q., Xie, P., Shen, H., Xu, J., Wang, P., and Zhang, B.: A novel flushing strategy for diatom bloom prevention in the lower-middle Hanjiang River, Water Res., 46(8), 2525-2534, https://doi.org/10.1016/j.watres.2012.01.051, 2012.

Yang, Y., Chen, S., Zhou, Y., Ma, G., Huang, W., and Zhu, Y.: Method for quantitatively assessing the impact of an inter-basin water transfer project on ecological environment-power generation in a water supply region, J. Hydrol., 618, 129250, https://doi.org/10.1016/j.jhydrol.2023.129250, 2023.

Zeng, Y., Liu, D., Guo, S., Xiong, L., Liu, P., Chen, J., Yin, J., Wu, Z., and Zhou, W.: Assessing the effects of water resources allocation on the uncertainty propagation in the water-energy-food-society (WEFS) nexus. Agric, Water Manag., 282, https://doi.org/10.1016/j.agwat.2023.108279, 2023.

Zhang, B.H.M.M.: Selection of installed capacity of Xinglong Hydropower Station, Hydropower and New Energy, (01), 66-68, https://doi.org/10.13622/j.cnki.cn42-1800/tv.2008.01.020, 2008.

Zhang, J., Bing, J., Li, X., Guo, L., Deng, Z., Wang, D., and Liu, L.: Inter-basin water transfer enhances the human health risk of heavy metals in the middle and lower Han River, China, J. Hydrol., 613, 128423, https://doi.org/10.1016/j.jhydrol.2022.128423, 2022.

Zhang, J., Xu, L., Yu, B., and Li, X.: Environmentally feasible potential for hydropower development regarding environmental constraints, Energy Policy, 73, 552-562, https://doi.org/10.1016/j.enpol.2014.04.040, 2014.

Zhao, D., Liu, J., Sun, L., Ye, B., Hubacek, K., Feng, K., and Varis, O.: Quantifying economic-social-environmental trade-offs and synergies of water-supply constraints: An application to the capital region of China, Water Res., 195, 116986-116986, https://doi.org/10.1016/j.watres.2021.116986, 2021.

Zhao, Z., Zuo, J., and Zillante, G.: Transformation of water resource management: a case study of the South-to-North Water Diversion project, J. Clean. Prod., 163, 136-145, https://doi.org/10.1016/j.jclepro.2015.08.066, 2017.

Zitzler, E.: Two decades of evolutionary multi-criterion optimization: A glance back and a look ahead, 2007 Ieee Symposium on Computational Intelligence in Multi-Criteria Decision Making, 318, https://doi.org/10.1109/MCDM.2007.369107, 2007.